**Orally -Bioavailable Androgen Receptor Degrader: Potential Next-Generation Therapeutic for Enzalutamide-Resistant Prostate Cancer**

Suriyan Ponnusamy[1], Yali He[2], Dong-Jin Hwang[2], Thirumagal Thiyagarajan[1], Rene Houtman[3], Vera Bocharova[4], Bobby G. Sumpter[4], Elias Fernandez[5], Daniel Johnson[6], Ziyun Du[7], Lawrence M. Pfeffer[7], Robert H. Getzenberg[8,#], Iain J. McEwan[9], Duane D. Miller[2], and Ramesh Narayanan[1,10,*]

[1] Department of Medicine, University of Tennessee Health Science, Memphis, TN

[2] Department of Pharmaceutical Sciences, University of Tennessee Health Science Center, Memphis, TN

[3] PamGene International, Den Bosch, The Netherlands.

[4] Oak Ridge National Laboratory, Oak Ridge, TN

[5] Biochemistry and Cell & Molecular Biology, University of Tennessee, Knoxville, TN

[6] Molecular Bioinformatics Core, University of Tennessee Health Science Center, Memphis, TN

[7] Department of Pathology, University of Tennessee Health Science Center, Memphis, TN

[8] GTx, Inc., Memphis, TN

# Current address. Dr. Kiran C. Patel College of Allopathic Medicine, Nova Southeastern University, Fort Lauderdale, FL

[9] Institute of Medical Sciences, School of Medicine, Medical Sciences and Nutrition, University of Aberdeen, Forester hill, Aberdeen, Scotland, UK

[10] West Cancer Center, Memphis, TN

* To whom correspondence should be addressed

Dr. Ramesh Narayanan
Department of Medicine
Division of Hematology and Oncology
University of Tennessee Health Science Center
Cancer Research Building
19, S. Manassas, Room 120
Memphis, TN-38103
Phone 901-448-2403
Fax. 901-448-3910
rnaraya4@uthsc.edu

**Disclosure**. RN is a consultant to GTx, Inc. This work was supported by a research grant from GTx, Inc. The SARD UT-34 described in the manuscript has been licensed to GTx, Inc. by the University of Tennessee Research Foundation.

**Translational relevance**: Conventional prostate cancer therapeutics are ligand binding domain (LBD)-binding competitive androgen receptor (AR) antagonists. Mechanistically-distinct new chemical entities that can provide sustained growth inhibition to the evolving forms of prostate cancer are required. Here, we describe the discovery and characterization of an AR degrader that inhibits the growth of prostate cancers that are not only sensitive but also resistant to competitive antagonists. Unlike competitive antagonists, the AR degrader inhibits the growth of prostate cancer xenografts grown in intact and castrated animals, suggesting that this agent can be used to treat both castration-resistant and androgen-dependent prostate cancer. With a broad safety margin, the molecule may offer a safe and effective treatment option for advanced prostate cancer.

**Abstract**: Androgen receptor (AR)-targeting prostate cancer drugs, which are predominantly competitive ligand binding domain (LBD)-binding antagonists, are inactivated by common resistance -mechanisms. It is important to develop next-generation mechanistically-distinct drugs to treat castration- and drug- resistant prostate cancers. Here, we describe a second-generation AR pan-antagonist (UT-34) that degrades the AR and AR splice variants. UT-34 inhibits the wild-type and LBD mutant ARs comparably and inhibits the *in vitro* proliferation and *in vivo* growth of enzalutamide-sensitive and resistant prostate cancer xenografts. In preclinical models, UT-34 induced the regression of enzalutamide-resistant tumors at doses when the AR is degraded; but, at lower doses when the AR is just antagonized, it inhibits, without shrinking, the tumors. This indicates that degradation might be a prerequisite for tumor regression. Mechanistically, UT-34 promotes a conformation that is distinct from the LBD-binding competitive antagonist, enzalutamide, and degrades the AR through the ubiquitin proteasome mechanism. UT-34 has a broad safety margin and exhibits no cross-reactivity with G-Protein Coupled Receptor, kinase, and nuclear receptor family members. Collectively, UT-34 exhibits the properties necessary for a next-generation prostate cancer drug.

**Key words**: Prostate cancer, castration-resistant prostate cancer (CRPC), androgen receptor (AR), AR degrader (SARD), coactivator, enzalutamide-resistant prostate cancer.

**Running title**: A novel AR degrader for the treatment of prostate cancer.

**Introduction**: About 3.3 million men are presently living with prostate cancer (PCa) in the United States and this number is expected to increase to 4.5 million by 2026 (1). In addition to radical prostatectomy combined with gonadotrophins, androgen-synthesizing enzyme inhibitor and androgen receptor (AR) antagonists have been the mainstay of PCa treatment (2,3). PCa that progresses after initial treatment (castration-resistant prostate cancer (CRPC)), grows rapidly and metastasizes to distant organs (4,5). Studies with targeted treatments (enzalutamide and apalutamide, AR antagonists, and abiraterone, an androgen-synthesizing enzyme inhibitor) that have been approved in the last 5-10 years to combat CRPC have provided clear evidence that CRPC, despite being castration-resistant, is still dependent on the AR axis for continued growth (2,3).

About 30-40% of CRPCs fail to respond to enzalutamide or abiraterone (2,3,6,7), while the remaining CRPCs eventually develop resistance after a brief period of response (8). Although several potential mechanisms for resistance development have been identified, mutations in the AR ligand binding domain (LBD), AR amplification, and expression of AR splice variants (AR-SVs) have been broadly observed in the clinic (9,10). AR antagonists currently in use (enzalutamide and apalutamide) and in clinical trials (darolutamide) are all competitive antagonists and their mechanisms of action are similar.

A member of the steroid receptor family of ligand-activated transcription factors, structurally, AR, like other steroid receptors, contains an N-terminus domain (NTD) that expresses an activation function (AF)-1 domain, a DNA-binding domain (DBD) that recognizes hormone

response elements, a hinge region, and an LBD that contains an AF-2 (11). The AF-1 contains two transcription activation regions, tau-1 and tau-5, which retain the majority of the AR function. Drugs that target the steroid receptors act by predominantly binding to the LBD. Prolonged treatment with AR antagonists results in mutations in the LBD, leading to resistance, i.e. W741 mutation leads to bicalutamide resistance (12), and F876 mutation confers resistance to enzalutamide and apalutamide (9,13,14).

While mutations in the AR-LBD can be ideally overcome with antagonists that bind to the LBD in a distinct conformation, resistance due to AR-SVs confers a serious challenge due to the absence of the LBD. Current AR-targeting drugs that bind to the LBD will be unable to inhibit AR-SV function. AR-SVs have been shown to be responsible for aggressive CRPC phenotype, shorter overall survival, and failure of the cancer to respond to AR-targeted treatments or to chemotherapeutic agents (10,15-18). Although most of the recent studies on PCa resistance have focused on AR-SVs, other pathways are also considered to play roles in resistance development (19,20).

Although degraders of estrogen receptor (ER) have been successfully discovered (21,22), AR degraders have not yet been developed. Degraders confer the added advantage of preventing AR activation by alternate signaling pathways and by intra-tumoral androgens, and hence might provide a sustained treatment option for CRPC. Since it is unclear whether the AR and AR-SVs exist as heterodimers or as independent homodimer isoforms, it is yet to be determined whether degrading the full length AR could contribute to the down-regulation of the AR-SVs (23,24).

Discovery of proteolysis targeting chimeras (PROTACs) and small molecules from our group has indicated that AR degraders could be developed using alternate strategies (25-28). However, PROTACs are large molecules with molecular weights greater than 1000 Da and our first-generation molecules (27,28) have poor oral bioavailability. It is also important to develop molecules that bind to domains other than the LBD (27,29) to inhibit AR-SVs and to overcome resistance.

Here we report the discovery of a novel small molecule pan-antagonist and degrader, UT-34, a second-generation molecule, that binds to the AR, and degrades enzalutamide-sensitive and –resistant ARs and AR-SVs. UT-34, which possesses appropriate pharmacokinetic (PK) properties, was effective in various *in vivo* models. UT-34 inhibited androgen-dependent tissues such as prostate and seminal vesicles in rats, and the growth of enzalutamide-resistant CRPC xenografts. UT-34 also induced tumor regression in intact immunocompromised rats, which has not been observed before with competitive antagonists potentially due to their inability to compete against the abundant circulating testosterone. These data provide the first evidence for the potential of an orally-bioavailable AR degrader to treat advanced prostate cancer.

**Materials and Methods**.

*Reagents.* The source of several reagents used in this manuscript has been described previously (27,28). The following reagents were purchased from the indicated vendors: $^{3}$H-mibolerone and R1881 (Perkin Elmer, Waltham, PA). Enzalutamide (MedKoo, Morrisville, NC). Dual-luciferase and CellTiter-Glo assay reagents (Promega, Madison, WI). AR (N20 and C19), mono-

and poly- ubiquitin (SC-8017), and glucocorticoid receptor (GR) antibodies (Santa Cruz biotechnology, Santa Cruz, CA). AR PG-21 antibody (Millipore, Burlington, MA). Dihydrotestosterone (DHT), dexamethasone, glyceraldehyde 3-phosphate dehydrogenase (GAPDH) antibody, chelerythrine chloride, and cycloheximide (Sigma, St. Louis, MO). Progesterone receptor (PR), estrogen receptor (ER), phospho PAK, and phospho PKC antibodies (Cell Signaling, Danvers, MA). Bortezomib and PAK inhibitor PF3758309 (Selleck Chemicals, Houston, TX). AR-V7 antibody and serum prostate specific antigen (PSA) kit (Abcam, Cambridge, UK). Lipofectamine and TaqMan primers and probes and real time polymerase chain reaction (PCR) reagents (Life Technologies, Carlsbad, CA). Hyaluronic acid (HA) antibody (Novus Biologicals, Littleton, CO). Doxycycline and 17-AAG (Fisher Scientific, (Hampton, NH). Liver microsomes (Xenotech LLC, Kansas City, KS). Proteasome inhibitor MG-132 (R&D Systems, Minneapolis, MN). On-target plus smart pool non-specific and MDM2 siRNA were obtained from Dharmacon (Thermo Fisher).

*Cell Culture.* LNCaP, PC-3, HEK-293, ZR-75-1, MDA-MB-453, VCaP, 22RV1, and COS7 cell lines were procured from the American Type Culture Collection (ATCC, Manassas, VA) and cultured in accordance to their recommendations. LNCaP cell line stably transfected with doxycycline-inducible AR-V7 was a kind gift from Dr. Nancy L. Weigel (Baylor College of Medicine, Houston, TX) (30,31). LNCaP95 prostate cancer cell line that expresses AR and AR-V7 was a kind gift from Dr. Alan Meeker (John Hopkins Medical Institute, Baltimore, MD) (32). Enzalutamide-resistant LNCaP (MR49F) cells were a kind gift from Dr. Martin Gleave (University of British Columbia, Vancouver) (33). Enzalutamide-resistant VCaP cells (MDVR) were licensed from Dr. Donald McDonnell (Duke University, NC). Patient-derived xenograft

(PDX) line PC346C was a kind gift from Dr. Van Veerden (University Medical Center, Roterdam) (34,35). All cell lines were authenticated by short terminal DNA repeat assay (Genetica, Burlington, NC).

*Gene expression.* RNA extraction and cDNA preparations were performed using Cells-to-Ct kit. Gene expression studies were performed using TaqMan probes on an ABI 7900 real time PCR system.

*Growth Assay.* Growth assay was performed using CellTiter-Glo or Sulfrhodamine blue (SRB) reagents.

*Plasmid constructs and transient transfection.* Plasmids (CMV hAR, AR-LBD, PR, GR, MR, ER, GRE-LUC, CMV-renilla LUC, AR-AF-1, and AR-NTD plasmids) used in the study were described earlier (27,36,37). Mouse AR, rat GR, GAA (GR-NTD, AR-DBD and AR-LBD), and AGG (AR-NTD, GR-DBD and GR-LBD) were kind gifts from Dr. Diane Robins (38). Constructs dtau1 (tau-1 deleted AR), dtau5 (tau-5 deleted AR), and AR-NTD-DBD were kind gifts from Dr. Frank Claessens (39,40). Transfections were performed using Lipofectamine reagent (Life Technologies, Carlsbad, CA).

*Competitive ligand binding assay*: Ligand binding assay with purified glutathione S transferase (GST)-tagged AR-LBD and whole cell binding assays with $^{3}$H-mibolerone were performed as

described previously (27,41). Briefly, COS7 cells were plated in 24 well plates at 100,000 cells/well in DMEM (without phenol red) supplemented with 5% charcoal dextran-stripped FBS (csFBS). Cells were transfected with the amounts of AR-LBD indicated in the figure. Cells were treated with a dose response of various compounds in the presence of $^{3}$H-mibolerone. Cells were washed four hours after treatment with ice cold PBS, and the intracellular proteins and $^{3}$H-mibolerone were extracted using ice cold 100% ethanol. Radioactivity was counted using a scintillation counter.

*Western blotting and immunoprecipitation.* Cells were plated in 60 mm dishes in growth medium. Medium was changed to the respective medium described in the figures and treated with compounds under various conditions. Protein extracts were prepared and Western blot was performed as described earlier (36,37). Immunoprecipitation was performed using protein A/G agarose.

*Fluorescence polarization (FP).* Endogenous steady-state emission spectra were measured for His-AR-NTD and His-AR-AF-1 purified proteins as described earlier (27,29,42).

*Micro array Assay for Real time Coregulator-Nuclear receptor Interaction (MARCoNI).* Functional AR analysis in cell lysates was performed as described previously (43,44). In short, compound-treated cells were harvested and lysed. Lysates, containing AR, were incubated on PamChip #88101 (PamGene, Den Bosch, The Netherland with 154 coregulator-derived NR-binding motifs, using 3 technical replicates (arrays) per lysate. AR binding was detected using a

fluorescently labeled antibody and quantified using BioNavigator software (PamGene). Treatment-induced log-fold change of coregulator binding (Modulation Index) treatment and p-value by Student's t-Test, both vs. vehicle-treatment, were calculated using R software and used to assess compound-induced modulation of AR conformation.

*Microarray*. To determine the effect of UT-34 on global gene expression, microarray analysis was performed. MR49F cells were maintained in 1% charcoal-stripped serum-containing medium for 2 days. Medium was changed again and the cells were treated with vehicle, 0.1 nM R1881 alone, or in combination with 10 μM UT-34 (n=3-4/group). At 24 hours after treatment, the cells were harvested, RNA extracted, and was subjected to microarray analysis (University of Tennessee Health Science Center (UTHSC) Molecular Resources Center). Clariom S array was processed as described previously (27) and the data was analyzed using One Way ANOVA. Genes that exhibited greater than 1.5 fold change with a false discovery rate $q<0.05$ were considered for further analysis. Ingenuity Pathway Analysis (IPA) was performed to determine the canonical pathway and the diseases represented by the enriched genes. The microarray data was deposited in Gene Expression Omnibus (GEO) database (accession number is GSE 133119).

*Mice Xenograft experiment*. All animal studies were conducted under UTHSC Animal Care and Use Committee approved protocols. Non obese diabetic/severe combined immunodeficiency Gamma (NSG) mice were housed five animals per cage and were allowed free access to water and commercial rodent chow. Cell line xenografts were performed in NSG mice as previously published (37,45). MR49F cells were implanted subcutaneously in intact mice (n=8-10/group). Tumors were measured twice or thrice weekly and the volume calculated using the formula

length*width*width*0.5236. Once the tumors reached 100-200 $mm^3$, the animals were castrated and the tumors were allowed to regrow as castration-resistant tumors. Once the tumors reached 200-300 $mm^3$ post castration, the animals were randomized and treated orally with vehicle (polyethylene glycol-300: DMSO 85:15) or UT-34. Animals were sacrificed at the end of the study and the tumors were weighed and stored for further processing.

*Rat xenograft experiments*. Rat xenograft experiments were performed in SRG (Sprague Dawley-Rag2:IL2rg KO) rats at Hera biolabs (Lexington, KY). Rats were inoculated subcutaneously with 10 X $10^6$ cells (VCaP or MDVR) in 50% matrigel. Once the tumors reached 1000-3000 $mm^3$, the animals were either randomized and treated (intact) or were castrated and the tumors were allowed to grow as CRPC. Once the tumors attain 2000-3000 $mm^3$, the animals were orally treated as indicated in the figures. Tumor volumes were recorded thrice weekly. Blood collection and body weight measurements were performed weekly. At sacrifice, tumors were weighed and stored for further analyses.

*Hershberger assay*. Male mice or rats (6-8 weeks old) were randomized into groups based on body weight. Animals were treated with drugs by oral administration as indicated in the figures for 4 or 14 days. Animals were sacrificed, prostate and seminal vesicles were weighed, and organ weights were normalized to body weight.

*Metabolic stability, pharmacokinetic (PK), safety, and cross-reactivity studies*. Metabolic stability studies in microsomes from various species were conducted as described previously

(27). PK studies were conducted at Covance (Madison, WI). Cross-reactivity of UT-34 with GPCRs, kinases, and nuclear receptors was evaluated at DiscoverX Eurofins.

*Statistics*. Statistical analysis was performed using *Prism* (GraphPad, San Diego, CA). T-test was used to analyze data from experiments containing two groups, while One Way analysis of variance (ANOVA) was used to analyze data from experiments containing more than two groups. Appropriate post hoc test was used to analyze data that demonstrated significance in ANOVA. Statistical significance is represented as * $p<0.05$; ** $p<0.01$; *** $p<0.001$.

LC-MS/MS method to detect UT-34 and UT-34 synthetic scheme are presented in the supplemental methods.

**Results**: Our first generation SARDs, UT-69 and UT-155, were excellent degraders with unique mechanistic properties (27). Unfortunately, their PK properties were not appropriate for further development. Oral administration of UT-155 in rats for 14 days failed to significantly inhibit the androgen-dependent seminal vesicles weight (**Figure S1A**). UT-155 when dosed orally failed to inhibit growth of enzalutamide-resistant LNCaP (MR49F) xenograft grown in castrated NSG mice (**Figure S1B**). Mouse and human liver microsomes data also show rapid clearance and short half-life of UT-155 (**Figure S1C**). Hence, we continued our pursuit to develop molecules that retain the degradation and antagonistic characteristics of the first- generation molecules but with better PK properties. UT-34 (**Figure 1A**), which satisfies these requirements was selected from a library for further characterization in order to develop it as a treatment for enzalutamide-resistant CRPC.

*UT-34 inhibits wild-type and mutant ARs comparably*. UT-34 was first tested in a binding assay *in vitro* using purified AR-LBD binding assay (27). Below 100 μM concentration, UT-34 failed to bind to the purified AR-LBD and displace 1 nM $^{3}$H-mibolerone (**Figure 1B left panel**). To verify the result obtained in purified AR-LBD, we performed whole cell ligand binding assays in COS7 cells transfected with AR-LBD and treated with a dose response of UT-34 in combination with 1 nM $^{3}$H-mibolerone. UT-34 displaced $^{3}$H-mibolerone, although its binding was much weaker (inhibition observed only at 10 μM) than that of enzalutamide or UT-155 (**Figure 1B right panel**). The ten-fold difference between purified AR-LBD and whole cell binding assays could be due to many possibilities: potential stabilization of the UT-34-AR-LBD complex by intracellular factors or faster on-off rate of UT-34 in the ligand binding pocket in the absence of stabilization factors, or requirement of additional factors to bind to the AR-LBD. These questions need to be resolved in future studies.

We next determined the antagonistic property of UT-34 in wild-type and LBD mutant ARs and compared the results to the effect of enzalutamide (**Figure 1C and Table ST1**). COS7 cells were transfected with wild-type or mutant ARs, GRE-LUC, and CMV-renilla LUC and a luciferase assay was performed. UT-34 and enzalutamide antagonized the wild-type AR with $IC_{50}$ around 200 nM. UT-34 inhibited the various mutant ARs (W741L, T877A, and F876L) comparably or with better $IC_{50}$. In contrast, enzalutamide was weaker in W741L by 5-fold, and behaved as a partial agonist in F876L AR (also partially antagonizes in the presence of androgens) as reported earlier (9,14). $IC_{50}$ value for enzalutamide in the antagonist mode could not be deduced due to its partial agonistic activity.

*UT-34 downregulates T877A-AR and F876L-enzalutamide-resistant AR*. As our objective was to develop degraders of the AR, we determined the effects of UT-34 on AR protein level in LNCaP cells and in enzalutamide-resistant MR49F cells as described in **Figures 2A and 2B**. LNCaP or MR49F maintained in charcoal-stripped serum-containing medium were treated with a dose response of UT-34 in the presence of 0.1 nM R1881 for 24 hours. Cells were harvested, protein extracted, and Western blotted for AR. While treatment of LNCaP cells with UT-34 resulted in a reduction of AR levels at 1000 nM (**Figure 2A left panel**), enzalutamide and bicalutamide failed to down-regulate the AR in LNCaP cells (**Figure 2A right panel**). These effects occurred without an effect on AR mRNA expression (**Figure 2A bar graph**). Similar to parental LNCaP cells, MR49F cells treated with UT-34 exhibited a significant reduction in AR levels at around 1000 nM, which is comparable to that observed in LNCaP cells (**Figure 2B**).

To demonstrate the selectivity of UT-34 to AR, the compound was tested in various cross-reactivity experiments. While UT-34 and enzalutamide failed to inhibit the transactivation of GR and mineralocorticoid receptor (**Table ST1**), UT-34 inhibited PR activity with a 4-5 fold weaker potency compared to the AR antagonistic activity.

To determine the degradation cross-reactivity of UT-34, we used various breast cancer cell lines that express AR and other steroid-hormone receptors. T47D that expresses ER and PR, but not AR, was used to evaluate the cross-reactivity of UT-34. T47D cells were maintained in serum-containing growth medium and treated with a dose-response of UT-34 in the absence of R1881 and Western blot for ER, PR, and actin was performed. UT-34 failed to down-regulate the ER

and PR protein levels (**Figure 2C**). Although some reports suggest that T47D cells express AR (46,47), our clone does not express AR.

To evaluate the cross-reactivity in a system that expresses AR, PR, and ER, we used ZR-75-1 breast cancer cells (48). Treatment of ZR-75-1 cells maintained in serum-containing growth medium with UT-34 resulted in down-regulation of AR protein levels, but not ER or PR levels (**Figure 2D**). Furthermore, in MDA-MB-453 breast cancer cells that express AR and GR (49,50), UT-34 induced the down-regulation of AR, but not GR (**Figure S2A**). This confirms that under similar condition UT-34 is selective to AR and does not degrade other receptors.

*UT-34 requires ubiquitin proteasome pathway to degrade the AR*. To determine if UT-34 promotes the ubiquitination of the AR, COS7 cells were transfected with AR and HA-tagged ubiquitin and treated with UT-155 or UT-34 in the presence of 0.1 nM R1881. UT-155 was used as positive control in these experiments. Ubiquitin was immunoprecipitated using HA antibody and Western blot for AR was performed. Western blot for AR with non-immunoprecipitated samples shows that both UT-155 and UT-34 down-regulated the AR (**Figure 2E input**). When ubiquitin was immunoprecipitated and AR was detected, the AR was both mono- and poly-ubiquitinated in the presence of UT-34 and UT-155 (**Figure 2E**). Similar results were also found in LNCaP cells treated with UT-155 or UT-34 (**Figure 2F**). The proteasome inhibitor MG132, but not the HSP90 inhibitor 17AAG, enriched the ubiquitinated AR in cells treated with UT-34 or UT-155.

To further characterize the requirement of the proteasome pathway for UT-34 to down-regulate the AR, LNCaP cells were treated with UT-34 and cycloheximide alone or in combination with a dose response of proteasome inhibitor bortezomib. UT-34 and cycloheximide combination down-regulated the AR and this down-regulation was reversed dose-dependently by bortezomib starting from 5 μM (**Figure 2G**). These results suggest that UT-34 requires ubiquitin proteasome pathway to degrade the AR.

We mutated the three known ubiquitin sites in AR (K311, K846, and K848) to arginine (R) and performed Western blots with protein extracts from cells transfected with wild-type and mutant ARs and treated with UT-34. UT-34 treatment facilitated the degradation of the wild-type and K-R mutant ARs comparably (**Figure 2H**), indicating that the known ubiquitin sites do not have a role in UT-34-dependent ubiquitin proteasome degradation. The effect of UT-34 on ubiquitination of the triple mutants needs to be evaluated.

To elucidate the signaling pathway that mediates the UT-34-dependent AR down-regulation, we explored signaling pathways, p21-activated kinase (PAK) and protein kinase C (PKC) that have already been shown to promote AR ubiquitination. Phosphorylation of $Ser^{578}$ by PAK has been demonstrated to be important for ubiquitin-dependent AR degradation. Moreover, since $Ser^{578}$ is a substrate of both PAK and PKC (51,52), we evaluated the role of these two pathways in UT-34-dependent degradation in LNCaP cells. Inhibition of PAK and PKC by small molecule inhibitors, PF-3758309 (53) and chelerythrine chloride (54), respectively, failed to reverse the down-regulation of AR by UT-34 (**Figure S2B**).

The ubiquitin E3 ligase that plays a role in AR's proteasomal degradation is MDM2 (52,55). Using MDM2 siRNA, we evaluated the role of MDM2 in UT-34-dependent AR down-regulation. LNCaP cells were transfected with MDM2 or non-targeting siRNAs and the expression of AR protein was determined by Western blot. MDM2 siRNA failed to block the UT-34-dependent AR down-regulation (**Figure S2C**). These results suggest that UT-34 down-regulates AR through a mechanism independent of PAK, PKC, or MDM2.

*UT-34 binds to AR-AF-1 domain*. The steady-state fluorescence emission spectra for proteins results from the presence of aromatic amino acids, with tryptophan fluorescence making the dominant contribution. The AR-NTD polypeptide contains 19 tyrosine (Y), clustering in the middle (amino acids 348 to 408) and towards the c-terminal region (amino acids 447 to 535), and four tryptophan residues (W399, 435, 503 and 527) (**Figure 3A top panel**). Excitation at 278 nm results in fluorescence emission from tryptophan and tyrosine residues; in addition, there can be energy transfer from tyrosine to tryptophan. The spectrum thus provides information about the local conformation surrounding these residues (27,56). The fluorescence spectrum for AR-AF1 is characterized by an emission maximum at 343 nm, due to the tryptophan residues ($W^{399,\ 435}$) and a shoulder at 309 nm, resulting from tyrosine emission (**Figure 3A, bottom left panel**). The folding or unfolding of AR-AF1/ NTD has been investigated using TMAO, which has been shown to facilitate the folding of proteins into "native" conformations (56). In the presence of up to 3 M TMAO there was blue shift in tryptophan emission maximum to 336 nm, and the shoulder due to tyrosine fluorescence was lost (**Figure 3A, bottom left panel**). In contrast, in the presence of urea, the tryptophan emission 'red shifts' to 351 nm and there is a clear peak for tyrosine emission. These results reflect the tryptophan residues becoming less or more solvent-

exposed respectively, and changes in the efficiency of energy transfer from tyrosine to tryptophan residues, consistent with the AR polypeptide folding/unfolding respectively.

In the presence of UT-34 there are some striking changes in the steady state emission spectra for both AR-AF1 and AR-NTD: all spectra were corrected for buffer and the presence of UT-34 alone. Increasing the concentration of UT-34 led to a peak at around 309 nm corresponding to tyrosine emission. Unlike our published data for UT-155, no clear quenching, reduction in the fluorescence emissions was observed in the presence of UT-34. Previously, quenching provided evidence for small molecule binding (27,29). The increase in the tyrosine signal is similar to that seen when AR-AF1/ NTD unfolds in the presence of urea, but there were no significant changes in the emission maximum for tryptophan (**Figure 3A, bottom right panel**). Although difficult to interpret, it seems likely that UT-34 binding may lead to local unfolding of the receptor polypeptides (resulting in tyrosine emission), without altering the solvent exposure of the tryptophan residues. These results were reproduced with AR-NTD (**Figure S2D**).

As UT-34 binds to both LBD and AF-1 domains and also promotes degradation of the AR, we sought to determine the domain that is required for UT-34 to degrade the AR. Since UT-34 selectively promoted AR degradation and not the GR, AR-GR chimeric receptors were used to evaluate the domain(s) important for the degradation. AR, GR, or AR-GR chimeric receptors were transfected into cells and the cells were treated with UT-34 in the presence of the respective hormones. As shown earlier, UT-34 promoted the degradation of the full-length AR, but not the GR (**Figure 3B**). UT-34 also promoted the degradation of the chimeric protein obtained from fusing AR-NTD to GR-DBD and -LBD (AGG), yet failed to promote degradation of the

chimeric protein obtained from fusing GR-NTD to AR-DBD and AR-LBD (GAA). These results suggest that UT-34 potentially requires NTD to facilitate AR degradation (**Figure 3B**).

To further refine the region in the AF-1 domain that is important for UT-34 to degrade the AR, a construct with the tau-5 domain deleted (tau-5 deleted AR) was used. COS7 cells were transfected with AR or tau-5-deleted AR, treated with vehicle or UT-34 for 48 hours, and a Western blot was performed for AR and GAPDH. UT-34 caused the degradation of the full-length AR, but not the tau-5-deleted AR (**Figure 3C**). Collectively, these data support UT-34 binding to the AR-NTD/AF-1 and the requirement of the Tau-5 region for the receptor degradation.

*UT-34 does not inhibit the AR function by competitive antagonism*. We then evaluated the early expression of pre-mRNAs in LNCaP cells treated with UT-34 in the presence or absence of R1881 (57). If UT-34 mediates its antagonistic effects through competitive antagonism, then these pre-mRNAs induced by R1881 as early as 30 minutes should be inhibited. However, if degradation is required for UT-34 to inhibit AR function, then early induction of the pre-mRNAs should not be inhibited as degradation will not be observed as early as 30 minutes to two hours. Treatment of LNCaP cells with 0.1 nM R1881 increased both NDRG1 and MT2A pre-mRNAs by one hour and the increase was sustained at two and 24 hours (**Figure 3D**). UT-34 failed to inhibit the expression of the pre-mRNA at one and two hours, yet inhibited the expression at 24 hours. These results indicate that UT-34 acts through AR degradation to elicit its effect, and competitive binding to the LBD, if any, may have no functional significance.

*UT-34 promotes AR-V7 degradation.* As the SARDs bind to the AF-1 domain and can promote AR-SV-degradation (27), we tested UT-34 in LNCaP cells that stably express inducible AR-V7 (30,31). Consistent with our previous results (27), UT-155 caused the degradation of the AR and AR-V7 in this system. UT-34 treatment down-regulated the AR and AR-V7, indicating that UT-34 is an effective degrader of both AR and AR-V7 (**Figure 3E**). Similar findings were observed in LNCaP-95 cells that express AR and AR-V7 (**Figure 3E**). These effects were observed without any effect on AR-V7 mRNA in LNCaP-ARV7 cells (**Figure 3E**).

As UT-34 caused the down-regulation of AR-V7, we evaluated the functional consequences of this down-regulation. LNCaP-ARV7 cells were treated as indicated in **Figure 4A** for 24 hours in the presence of 0.1 nM R1881 or 10 ng/ml doxycycline. Cells were harvested and the expression of AR-target gene FKBP5 and an AR-V7-specific gene EDN2 (30,31) was measured by real time PCR. Doxycycline induced the expression of EDN2, which was inhibited by UT-34, but not by enzalutamide, while both enzalutamide and UT-34 inhibited the expression of R1881-induced FKBP5 gene expression (**Figure 4A**).

*UT-34 differentially modulates AR-cofactor interaction compared to enzalutamide*. To determine if the properties of UT-34 are a result of a distinct interaction of AR with cofactors, we treated serum-starved LNCaP cells with 10 μM UT-34, UT-155, or enzalutamide or vehicle in the presence of 1 nM DHT. The cells were pretreated with the drugs or vehicle for 2 hours, followed by a 30 minutes treatment with DHT. Protein extracts were subjected to MARCoNI assay where the interaction of the AR with 154 unique cofactor peptides from 66 cofactors was evaluated (43). UT-34 and UT-155 significantly modulated the AR-cofactor interaction (**Figure 4B top**

**panel**). Although, the interaction between AR and cofactors in the presence of UT-155 and UT-34 was largely similar to enzalutamide (although with reduced potency), some differences were also observed (**Figure 4B bottom panel and table**). Differences in the interaction of AR with cofactors such as NCoR1 (corepressors) and TREF1 (coactivator) observed in SARD-treated samples were not observed in cells treated with enzalutamide. These results indicate that the conformation of AR in the presence of the SARDs is modestly distinct from the conformation in the presence of a competitive antagonist such as enzalutamide. The results from this cofactor profiling, as reflected by the conformation change, provide minimal mechanistic evidence for the UT-34's AR degradation effect. Further studies need to be performed to definitely determine if the cofactor profile observed with UT-34 or UT-155 is an indicator of the conformation that is required to degrade the AR.

*UT-34 antagonizes enzalutamide-resistant AR and inhibits the proliferation of enzalutamide-resistant MR49F cells*. As UT-34 robustly antagonized and degraded wild-type, T877A, and enzalutamide-resistant ARs in transient transactivation and Western blot assays, we evaluated the effect of UT-34 on the function of ARs expressed in LNCaP or MR49F cells. LNCaP cells were maintained in charcoal-stripped FBS-containing medium for 48 hours and treated with a dose-range of UT-34 or enzalutamide in the presence of 0.1 nM R1881. RNA was isolated and expression of AR target genes and growth was evaluated. Both the compounds inhibited the expression of PSA and FKBP5 and growth of LNCaP cells starting from 100 nM with maximum effect observed at 10 μM (**Figure 5A**).

The experiment was also performed in MR49F cells that express F876L mutant AR. UT-34, but not enzalutamide, inhibited the expression of FKBP5 gene induced by R1881 (**Figure 5B**). Concomitant to the gene expression studies, UT-34 inhibited the proliferation of MR49F cells, while as expected enzalutamide failed to inhibit their proliferation. The anti-proliferative effects of UT-34 are selective to AR-positive prostate cancer cells, as UT-34 did not have any effect on the proliferation of AR-negative PC-3, COS-7, and HEK-293 cells (**Figure S3A**).

*UT-34 inhibits AR-function and proliferation of an AR-amplified model (VCaP cells), and a PDX model*. One of the mechanisms for CRPC development and for resistance to AR antagonists, bicalutamide in particular, is AR amplification (58-60). LNCaP cells ectopically over-expressing AR was used as a screening tool to discover and characterize enzalutamide and apalutamide (61). While bicalutamide was inactive or even behaved as an agonist in this model, enzalutamide was effective in reducing the LNCaP-AR cell proliferation and AR-function (61). To test UT-34 in a model that has AR amplification, we used VCaP cells that endogenously expresses 10-fold higher AR than LNCaP cells (60). Earlier studies have shown that VCaP expresses 10-fold higher AR than parental LNCaP and 2-3 fold more than LNCaP-AR cells (60). Prior studies have also shown that bicalutamide is inactive or even functional as an agonist in this model (62,63). Western blot for AR expression in VCaP and LNCaP cells confirmed the AR amplification in VCaP cells compared to LNCaP cells (**Figure 5C**). VCaP cells maintained in charcoal-stripped serum-containing medium for two days were treated with 3 and 10 μM UT-34, enzalutamide, or bicalutamide in the presence of 0.1 nM R1881 and the expression of AR-target genes was measured (**Figure 5C**). R1881 induced the expression of AR-target genes, FKBP5 and TMPRSS2, and this induction was inhibited by UT-34 and enzalutamide, but not by

bicalutamide. Also, UT-34 and enzalutamide, but not bicalutamide, inhibited the proliferation of VCaP cells after 9 days of treatment (**Figure 5C**). These results were confirmed in enzalutamide-resistant VCaP, MDVR cells (**Figure S3B**). These results suggest that, unlike bicalutamide, the effect of UT-34 is not weakened by AR amplification.

UT-34 was also evaluated in a PDX cell line PC346C that expresses AR at levels comparable to LNCaP (**Figure 5D**). PC346C cells maintained in growth medium were treated with 3 and 10 μM of UT-34 or enzalutamide and expression of AR-target gene FKBP5 was measured. UT-34 and enzalutamide inhibited FKBP5 expression, with UT-34 demonstrating a slightly better response than enzalutamide. Concurrent with the gene expression findings, UT-34 significantly inhibited the proliferation of PC346C cells.

*UT-34 inhibits R1881-induced gene expression in MR49F cells*. As UT-34 was effective in inhibiting the expression of FKBP5 in MR49F cells, we performed a microarray experiment to determine the effect of UT-34 on R1881-induced global gene expression (**Figure 5E left**). The resulting heatmap clearly illustrates that R1881 robustly altered the expression of approximately 700 genes. Most, if not all, of the genes regulated by R1881 were reversed by UT-34 almost to the level observed in vehicle-treated cells. The top genes that were inhibited by UT-34 are all known AR-target genes such as FKBP5, SNAI2, NDRG1, and others. The results indicate that UT-34 is effective in reversing the R1881 effect in LNCaP cells expressing enzalutamide-resistant AR. Principal Component Analysis (PCA) shows that the UT-34-treated samples cluster with vehicle-treated samples, while R1881-treated samples clustered distinctly. When the genes that were not regulated by R1881 were plotted in a separate heatmap, the results show that UT-

34 has no effect on these genes (**Figure 5E right**), indicating that UT-34 effects are highly selective to the AR pathway with no off-target effects.

Ingenuity Pathway Analysis (IPA) results indicate that the top four canonical pathways that were enriched in the differentially-regulated genes were cholesterol-synthesizing pathways (**Figure 5F**). While all genes in the pathway were up-regulated by R1881 treatment, UT-34 efficiently reduced their expression to the vehicle-treated control levels. IPA also indicates that genes in genitourinary oncology pathways are differentially regulated, validating the model that was used to generate the gene expression data.

*Drug metabolism and pharmacokinetic (DMPK) studies suggest that UT-34 is stable*. Due to short half-life ($T_{1/2}$) of the first-generation SARDs, UT-155 and UT-69, in mouse liver microsomes (MLM; primary pharmacodynamics (PD) species) (27), they had to be administered subcutaneously to obtain efficacy in preclinical models. Since CRPC is a chronic disease requiring prolonged treatment, orally bioavailable molecules are preferred for clinical development. Using MLM assay to determine the $T_{1/2}$ and intrinsic clearance, UT-34 was found to have a longer $T_{1/2}$ and lower intrinsic clearance than UT-155 (**Table ST2**). This suggests that UT-34 is an appropriate molecule for further development. Assessing the metabolism of UT-34 in rat liver microsome (RLM) and in human liver microsome (HLM), UT-34 was found to be highly stable and by at least 2-4 fold longer than in MLM.

To validate the *in vitro* data *in vivo*, the bioavailability of UT-34 at six and 24 hours after administration was determined in various strains of rats and mice (**Table ST3**). UT-34 was

highly bioavailable in mice and rats at six hours. However, the serum concentration precipitously decreased at 24 hours in mice to almost undetectable levels, while higher levels in µM range was still observed in rats at 24 hours. A PK study was conducted in rats that were administered 100-1000 mg/kg of UT-34 and the serum concentration was measured over a period of 24 hours. UT-34 was extremely stable in rats with $T_{1/2}$ for the 100 and 300 mg/kg doses undeterminable due to lack of 50% reduction by 24 hours and the serum concentrations in the range of 10-50 µM (**Figure S4A**). These results are in concordance with the results observed in liver microsomes. Lower dose PK of UT-34 in rats also provided similar results with UT-34 demonstrating stability up to 24 hours (**Figure S4B**).

*Pharmacodynamic and xenograft studies suggest that UT-34 is efficacious*: To determine the efficacy of UT-34 *in vivo*, a Hershberger assay was performed in mice and rats (**Figure S4C**). Mice (left panel) were administered with 20 or 40 mg/kg UT-34 or 30 mg/kg enzalutamide orally for 14 days. The animals were then sacrificed and the weight of the seminal vesicles was recorded. Enzalutamide was not dosed higher than 30 mg/kg due to its poor solubility. UT-34 at 20 and 40 mg/kg reduced the seminal vesicles weight by 10-20 % and 50-60 %, respectively, while enzalutamide reduced the seminal vesicles weight by 50% (**Figure S4C left panel**).

Sprague Dawley rats were dosed with 40 and 60 mg/kg of UT-34 orally and enzalutamide at 30 mg/kg for 14 days and the weight of the prostate was recorded. UT-34 reduced the prostate weight by ~70-80%, while enzalutamide reduced the prostate weight by 40-60%. This clearly shows that UT-34 is potent in shrinking the prostate potentially due to its antagonistic and degradation effects (**Figure S4C middle panel**). Even after just four days of dosing, UT-34

reduced the prostate weight by nearly 50%, indicating its ability to antagonize the AR quickly *in vivo* and produce a PD effect (**Figure S4C right panel**).

To evaluate the effect of UT-34 in an enzalutamide-resistant xenograft model, MR49F cells were implanted subcutaneously in NSG mice and once the tumors attained 100-200 $mm^3$, the animals were castrated and the tumors were allowed to regrow as CRPC. The animals were treated with 30 or 60 mg/kg UT-34 and the tumor volume was measured thrice weekly (**Figure 6A**). UT-34 dose-dependently decreased the growth of the enzalutamide-resistant CRPC tumors with 60 mg/kg producing ~ 75% tumor growth inhibition. Tumor weights recorded at the end of the study also indicated that UT-34 reduced the tumor weights by ~ 60-70% (**Figure 6A right panel**). Although the PK properties in mice were sub-optimal compared to rats, UT-34 produced a marked effect on enzalutamide-resistant tumor growth.

*UT-34 promotes regression of enzalutamide-sensitive and –resistant VCaP tumors in SRG rats*. Since UT-34 is stable in rats compared to mice, we performed xenograft studies in immunocompromised rats (Hera Biolabs, KY), using two models, enzalutamide-sensitive parental VCaP cells and enzalutamide acquired-resistant VCaP cells (MDVR). The rationale to choose VCaP over other models is a result of the relatively high AR expression (AR amplification), which is observed in a large percentage of men with CRPC (59). Cells were implanted in immunocompromised SRG rats and once the tumors reached a volume of 1000-3000 $mm^3$, the animals were castrated and the tumors were allowed to regrow as castration-resistant prostate cancer. Once the tumors reached >2000 $mm^3$, the animals were randomized and treated orally with vehicle, 30 mg/kg enzalutamide, or 60 mg/kg UT-34. Tumor volume

measurements indicated that while enzalutamide inhibited the growth of parental VCaP xenograft by >85%, UT-34 reduced the tumors to unmeasurable levels (**Figure 6B**).

As expected, enzalutamide failed to inhibit the MDVR xenograft. The anticancer activity of UT-34 in this tumor model was comparable to that observed in the parental VCaP xenograft with UT-34 reducing the tumors to unmeasurable levels (**Figure 6C**).

Since UT-34 reduced tumors to undetectable levels, we hypothesized that this could be due to its AR degrading activity. Western blot of MDVR tumors demonstrated AR degradation in UT-34-treated samples compared to vehicle-treated samples (**Figure 6C**).

Previous studies with competitive AR antagonists were unable to demonstrate inhibition of tumors grown in intact mice. Since UT-34 is an orally-bioavailable degrader, we were interested in testing the efficacy in intact models, where the animals were not castrated and the tumors were grown in the presence of circulating androgens. MDVR tumors grew robustly in SRG rats and the tumor-bearing animals were treated when the tumors attained >1500 $mm^3$. One tumor in each group even attained 10,000 $mm^3$ when treatment was initiated. While the vehicle- and enzalutamide- treated tumors grew robustly, UT-34-treated tumors were reduced by >50% in less than 10-15 days after treatment initiation (**Figure 6D individual tumors shown**). We then measured serum PSA to determine if tumor volume correlated with PSA levels. While PSA levels rose in vehicle-treated rats, UT-34 completely reduced serum PSA to undetectable levels after treatment initiation (**Figure 6D**).

We subsequently conducted a dose response of UT-34 in intact SRG rats bearing MDVR tumors. UT-34 at 10 mg/kg inhibited the tumors by >50% and completely inhibited the tumors at 20 and 30 mg/kg doses (**Figure 6E**). Both tumor weights and serum PSA at the end of the study clearly exhibited a dose-dependent inhibition by UT-34 (**Figure 6E**). Measurement of drug concentration in the serum and tumor at necropsy, which was collected 24-30 hours after last dosing demonstrated UT-34 accumulation in both serum and tumor at over 1-3 μM concentrations (**Figure S4D**). The steady-state drug concentration even 24 hours after the last dose is well above the $IC_{50}$ values of UT-34 to inhibit the AR. Immunohistochemistry of vehicle- and UT-34–treated (30 mg/kg) specimens clearly indicated that UT-34 increased the apoptosis as measured by TUNEL assay and inhibited the proliferation as measured by Ki67 staining (**Figure S4E**). Taken together these findings favorably point to the excellent anti-tumor activity of UT-34 in enzalutamide-sensitive and resistant prostate cancers even in intact non-castrated animals. No visible changes in H&E staining were observed (**Figure S5**).

To determine if the AR is degraded by UT-34 in intact conditions, we measured the AR expression by Western blot in protein extracts from tumors (**Figure 6D**). UT-34 robustly promoted degradation of the enzalutamide-resistant AR in intact condition (**Figure 6D**), demonstrating that the degradation property translates *in vivo*. We also evaluated whether UT-34 promoted degradation of the AR at lower doses. Unfortunately, UT-34 failed to promote AR degradation at 30 mg/kg (**Figure 6E**). This potentially suggests that higher serum and tumor concentrations are required to degrade the AR and that a tumor regression can be achieved only when the AR is degraded.

High doses of some receptor antagonists in certain cellular conditions could result in agonistic activity in artificial reporter assays. To ensure that UT-34 is a pure antagonist and does not have any agonistic activity at high doses, we tested UT-34 *in vivo* in castrated mice. Vehicle or UT-34 (100 mg/kg) was administered orally for 30 days to castrated mice, and seminal vesicles weights were recorded. Seminal vesicles are highly androgen-sensitive and any agonistic activity will increase its weight. Seminal vesicles weight normalized to body weight is expressed as percent change from vehicle control (**Figure S4F**). Even a high dose of UT-34 did not exhibit any agonistic activity as the normalized seminal vesicles weights in UT-34-treated group were comparable to weights of the vehicle-treated animals. Serum levels of UT-34 at the end of 30 days of dosing was in the range of 5-30 μM (**Figure S4F right panel**). These results confirm that UT-34 is a pure antagonist and does not have any agonistic properties *in vivo* even at higher doses.

*UT-34 toxicity profile was acceptable*: Since UT-34 possessed the required properties for a CRPC drug, we evaluated its toxicity profile. UT-34 was administered at 100, 300, and 600 mg/kg doses for seven days in Sprague Dawley rats and survival and gross pathology were monitored. UT-34 did not cause any death at 100 mg/kg dose, while deaths were encountered at 300 and 600 mg/kg doses. Gross pathology and histopathology findings suggest that the deaths in the higher dose groups were due to gastric irritation and inflammation, which could be potentially avoided by using enteric-coated capsules or salt forms of UT-34 (as UT-34 is a base). No other pathological observations were detected at any dose. While several of the second-generation AR antagonists exhibit seizure potentials, mice treated with UT-34 did not have any seizure. In addition, UT-34 also does not have any significant cross-reactivity with GPCRs,

kinases, or other nuclear receptors (Eurofin DiscoverX) and does not inhibit the hERG ion channel (Covance). These results suggest that UT-34 has a large safety margin and does not have off-target effects.

**Discussion**. Our results provide evidence for an orally bioavailable SARD that has the necessary drug-like properties for further clinical evaluation. UT-34 down-regulated the AR and AR-V7 splice variant, antagonized enzalutamide-sensitive and resistant AR, inhibited proliferation of AR-amplified cells, and inhibited the growth of enzalutamide-resistant xenografts. UT-34 also possesses appropriate metabolism properties showing longer half-life, and shorter clearance in rat and human liver microsomes than in mouse liver microsomes. This suggests that UT-34 might require only once daily dosing for clinical efficacy.

UT-34 is effective in two models of enzalutamide-resistance (AR-LBD mutation and AR-V7 expression), which are common forms of resistance observed clinically. Although 30% of enzalutamide-resistant cancers do not respond at all, the remaining cancers eventually develop resistance after treatment. Mutations constitute only a small fraction of the resistance, while AR-SV development, intra-tumoral androgen synthesis, AR amplification, coactivators, and altered intracellular signaling pathways all contribute to resistance development. Degrading the AR and AR-SVs will block any AR activation by these contributing factors providing a significant advantage over existing therapeutics. Recently, two AR inhibitors, galeterone and EPI-506, failed in the clinic. After the approval of enzalutamide and abiraterone in 2012, no other drugs targeting the AR with distinct mechanism of action (apalutamide was approved recently, but it is structurally and functionally similar to enzalutamide) have been made available and patients

have no treatment options with distinct mechanisms available to treat the new evolving forms of CRPC. Hence, these SARDs might provide a substantial advantage to the patients who relapse from enzalutamide.

We demonstrate that UT-34 promotes AR degradation through the ubiquitin proteasome pathway, the pathway by which most proteins are degraded. As AR degraders have not been successfully identified, thorough characterization of UT-34's mode of action is important. Unlike the ER degraders that act through the ER-LBD, UT-34 and its related compounds such as UT-155 act through the AR AF-1 domain in the N-terminus of the AR. UT-34 treatment resulted in mono- and poly- ubiquitinated AR. Also, inhibition of the proteasome pathway with bortezomib resulted in the reversal of AR degradation suggesting that the degradation takes place through proteasome pathway. Although recently available chimeric molecules such as PROTACs and SNIPERs have been shown to promote AR degradation (25,64), these molecules are larger than the normally desired 500 Da size for clinically useful pharmacologic agents. Since UT-34 degrades the AR-SVs and the well-characterized ubiquitin sites in the AR did not play a role in AR degradation by UT-34 (**Figure 2H**), UT-34 might act through novel ubiquitin sites in the AR-NTD that need to be identified.

This is the first time that an AR-targeting molecule has been shown to exhibit efficacy in xenograft models grown in intact (non-castrated) rodents. Since circulating testosterone levels are too high to be competed out with competitive antagonists, only non-competitive antagonists or degraders can inhibit tumor growth in intact animals. The results observed in enzalutamide-resistant MDVR xenografts in intact rats is an *in vivo* confirmation that UT-34 might be a non-

competitive antagonist. Moreover, the dose response and higher dose xenograft studies also suggest that tumor regression was obtained when the AR is degraded and not when just antagonized. These results are the first evidence of efficacy of orally- bioavailable small molecule AR degraders.

The mechanism by which AR interacts with its cofactors in the presence of a degrader or in the presence of a molecule that binds to a distinct domain and that does not function as a competitive antagonist has not been elucidated. We conducted the study in LNCaP prostate cancer cells as opposed to the *in vitro* system followed by others (65). Both UT-34 and UT-155 promoted the interaction of several cofactors with the AR similar to that of a competitive antagonist enzalutamide, yet distinct interactions were observed in the presence of the two degraders. These interactions will be followed in the future with a library of compounds to validate the results.

Although the first-generation AR degraders, UT-155, UT-69, and others (27,28), were more potent than UT-34 *in vitro* they were not orally bioavailable and their metabolism properties were not appropriate for drug development. Therefore, we had to compromise on the degradation and antagonist properties to improve the metabolism, which has resulted in a molecule that withstood various tests of efficacy and safety. Although a concern with AR-targeted drugs is seizure potential, UT-34 did not exhibit any seizure effects in rodents.

One of the intriguing properties of UT-34 is the difference in its PK between rats and mice. While the molecule was rapidly metabolized in mice, it was stable in rats. Based on the positive correlation between the liver microsome and PK properties in our data set, we expect UT-34 to

have similar, if not better, PK properties in humans. Although this species difference is an interesting observation, differences in PK properties between closely related species and between genders within a species have been reported previously (66,67). The mechanism for such differences between closely-related species or between genders within a species has not yet been elucidated.

UT-34 represents a new generation of orally-bioavailable molecule that possesses necessary characteristics of AR degraders, warranting clinical development. We expect UT-34 to overcome enzalutamide resistance in the clinic without having to worry about some of the common safety problems.

**Acknowledgement**. BGS acknowledges work performed at the Center for Nanophase Materials Sciences, a DOE Office of Science User Facility. VB acknowledges Laboratory Directed Research and Development program of Oak Ridge National Laboratory, managed by UT-Battelle, LLC, for the U.S. Department of Energy.

## Figure Legends

**Figure 1**: **Structure and properties of UT-34**. **A**. *Structure of UT-34*. **B left panel**. UT-34 does not bind to the AR-LBD. Purified GST-tagged AR-LBD protein was incubated for 16 hours at 4°C with a dose response (1 pM to 100 μM) of the indicated compounds in the presence of 1 nM $^{3}$H -mibolerone. Unbound $^{3}$H was washed and the bound $^{3}$H was counted using a scintillation counter. **B right panel**. COS7 cells were transfected with 50 ng of AR-LBD. Cells were treated 48 hours after transfection with a dose response (1 pM to 10 μM) of the indicated compounds in

the presence of 1 nM $^{3}$H-mibolerone for 4 hours. Unbound $^{3}$H-mibolerone was washed with cold PBS and the bound $^{3}$H was eluted with ice cold ethanol. $^{3}$H was counted using a scintillation counter. **C**. *UT-34 comparably inhibits the transactivation of wild-type and mutant ARs*. COS7 cells were transfected with 25 ng of cmv-hAR, hAR F876L, or hAR W741L, 0.25 µg GRE-LUC, and 10 ng CMV-renilla LUC using lipofectamine. Cells were treated 24 hours after transfection with a dose response of UT-34 or enzalutamide in combination with 0.1 nM R1881 (F876L agonist experiment was performed in the absence of 0.1 nM R1881) and luciferase assay was performed 48 hours after transfection. Firefly luciferase was divided by renilla luciferase. Values shown in the graphs are $IC_{50}$ values. Experiments were performed at least n=3 times and the representative graph is shown here. DHT – dihydrotestosterone; AR-androgen receptor; LBD-ligand binding domain; GST-glutathione S transferase RLU-Relative Light Units.

**Figure 2**: **UT-34 selectively degrades T877A and enzalutamide-resistant ARs**. **A**. *UT-34 destabilizes T877A AR*. LNCaP cells were maintained in 1% charcoal-stripped serum-containing medium for two days. Cells were treated with the indicated doses of UT-34 or enzalutamide or bicalutamide (right panel; enzalutamide and bicalutamide were used at 10 µM) in the presence of 0.1 nM R1881 for 24 hours, protein was extracted, and Western blot for AR and actin was performed. Lower bar graph shows no effect of UT-34 on AR mRNA expression under the same experimental conditions. **B**. *UT-34 destabilizes enzalutamide-resistant AR*. Enzalutamide-resistant LNCaP cells (MR49F) were cultured and treated as indicated for LNCaP cells. Western blot for AR and actin was performed with the protein extracts. **C-D**. *UT-34 selectively degrades the AR*. **C**. T47D cells maintained in full serum-containing medium were treated as indicated in the figure with UT-34. At 24 hours after treatment, cells were harvested, protein extracted, and Western blot for PR, ER, and actin was performed. **D**. ZR-75-1 cells were maintained in serum-

containing growth medium and were treated as indicated in the figures for 48 hours with cells retreated after 24 hours. Cells were harvested and Western blot for AR, PR, ER, and GAPDH was performed. **E**. *UT-34 promotes ubiquitination of the AR*. COS7 cells were transfected with 1 µg cmv-hAR and HA-ubiquitin. Cells were treated 48 hours after transfection for six hours. Cells were harvested, protein extracted, and immunoprecipitation for HA and Western blot for AR were performed. 10% of the protein extract was loaded as input. **F**. *UT-34 promotes ubiquitination of the AR in LNCaP cells*. LNCaP cells maintained in 1% charcoal-stripped serum-containing medium for two days were treated with UT-34 or UT-155 in the presence or absence of proteasome inhibitor, MG-132 and HSP-90 inhibitor, 17AAG, for six hours. Immunoprecipitation for AR was performed with the protein extract and Western blot with mono- and poly- ubiquitin antibody was performed. **G**. *UT-34 degrades the AR by proteasome pathway*. LNCaP cells plated in growth medium were treated as indicated in the figure for 8 hours. Western blot for AR and GAPDH was performed in the protein extracts. The blots were quantified and the numbers are represented under the Western image. **H**. *Known ubiquitin sites do not play a role in UT-34-induced degradation of the AR*. COS7 cells were transfected with 1 µg of wild-type AR or AR where three lysines (K311, K846, K848) were mutated to arginine (K to R). Cells were treated 24 hours after transfection for 24 hours and Western blot for AR and GAPDH was performed. Experiments were performed at least n=3 and representative blots are shown here. AR-androgen receptor; PR-progesterone receptor; ER-estrogen receptor; IP-immunoprecipitation; IB-immunoblot (Western blot); Ub-ubiquitin; cyclohex-cycloheximide-protein-synthesis inhibitor; Enza-enzalutamide; Bic-bicalutamide.

**Figure 3**. **UT-34 interacts with AR AF-1 domain. A**. **Top**. Schematic representation of the full-length human AR and the AR-NTD and -AF1 polypeptide. The location of tryptophan

residues (399, 435, 503 and 527) and 19 tyrosines are indicated. **Bottom left panel**, steady state fluorescence emission spectra for purified AR-AF1 (1 μM) in buffer or the presence of the osmolyte TMAO or the denaturant urea. Emission maxima for tryptophan (W) and tyrosine (Y) are indicated. **Bottom Right panel**, AR-AF-1 purified protein (1 μM) and increasing concentrations of UT-34 were pre-incubated for at least 30 minutes and steady state fluorescence was measured. The emission spectra were all corrected for buffer and presence of UT-34 and plotted relative to tryptophan emission maximum set to 100. **B**. *UT-34 degrades chimeric protein that expresses AR-NTD*. COS7 cells were transfected with 2.5 μg of the indicated constructs (AGG-AR-NTD, GR-DBD and LBD; GAA-GR-NTD, AR-DBD and LBD) and HA-ubiquitin. Cells were treated 24 hours after transfection and harvested 24 hours after treatment. Western blot for AR and GAPDH (left panel) and GR and GAPDH (right panel) was performed. **C**. *Tau-5 domain of the AR is important for UT-34-dependent degradation.* COS7 cells were transfected with 2.5 μg of the indicated constructs and HA-ubiquitin and Western blot for AR using AR C19 antibody and GAPDH was performed. **D**. *UT-34 does not inhibit early induction of NDRG1 and MT2A pre-mRNAs*. LNCaP cells maintained in charcoal-stripped serum-containing medium for 2 days were treated as indicated in the figures in triplicates. Cells were pre-treated with 10 μM UT-34 for 30 minutes before treatment with 0.1 nM R1881. Cells were harvested, RNA isolated, and the expression of various pre-mRNAs was measured at the indicated time-points. **E**. *UT-34 degrades AR-SV*. LNCaP-AR-V7 cells (LNCaP cells that stably express doxycycline-inducible AR-V7; left panel) or LNCaP-95 cells (middle) were maintained in charcoal-stripped serum-containing medium for 2 days. Doxycycline (10 ng/ml) was added to the LNCaP-AR-V7 cells during this period to induce the AR-V7 synthesis. After two days, medium was changed and the cells were treated with the indicated doses of UT-34 (UT-155 was used as a positive control in

the left panel) for 24 hours. Protein was extracted and Western blot for the AR and GAPDH was performed. Bar graph shows the lack of effect on AR-V7 mRNA in the presence of UT-34 under similar conditions. All the experiments were repeated three times and a representative experiment is presented here. AR-androgen receptor; GR-glucocorticoid receptor; NTD-N terminus domain; DBD-DNA binding domain; Hin-Hinge; LBD-ligand binding domain; Dex-dexamethasone; AGG-AR NTD, GR DBD and LBD; GAA-GR NTD, AR DBD and LBD.

**Figure 4**: **UT-34 inhibits AR and AR-V7-target gene expression and induces distinct AR conformation**. **A**. *UT-34 inhibits AR and AR-V7-target gene expression*. LNCaP-AR-V7 cells were maintained in charcoal-stripped serum-containing medium for 2 days. Cells were treated as indicated in the figure with 10 μM of the compounds in the presence of 0.1 nM R1881 or 10 ng/ml doxycycline (cells were pre-treated with UT-34 for 30 minutes for combination with R1881 and for 24 hours for combination with doxycycline). Twenty four hours after treatment initiation the cells were harvested, RNA isolated, and the expression of FKBP5 or EDN2 was determined by real time PCR. Gene expression values were normalized to the expression of GAPDH. * $p<0.05$. Values are expressed as average ± S.E. (n=3). **B**. *UT-34 and UT-155 alter the conformation of the AR*. LNCaP cells maintained in charcoal-stripped serum-containing medium for 2 days were treated with vehicle or 10 μM of the indicated compounds in the presence of 1 nM DHT (cells were pre-treated for two hours). Cells were harvested 30 minutes after DHT treatment and the pellets were shipped to PamGene. AR was immunoprecipitated and cofactor profiling was done in accordance with the previously published protocols. List of proteins different in the SARD-treated samples from enzalutamide-treated samples is provided in

the table below. Values represented are average of n=3 technical replicates. Enza-Enzalutamide; Veh-vehicle.

**Figure 5**: **UT-34 inhibits enzalutamide-sensitive and -resistant AR-dependent gene expression and prostate cancer cell proliferation**. **A**. *UT-34 inhibits the expression of AR-target genes in LNCaP cells*. LNCaP cells maintained in charcoal-stripped serum-containing medium for two days were treated with a dose response of UT-34 or enzalutamide in the presence of 0.1 nM R1881. RNA was isolated 24 hours after treatment and the expression of PSA and FKBP5 was quantified and normalized to GAPDH using real time PCR primers and probes. For the growth assay (right panel), cells were maintained and treated as indicated above for the gene expression studies, but were treated for six days with medium change and retreatment after three days. Sulforhodamine B (SRB) assay was performed to determine the number of viable cells. **B**. *UT-34 inhibits the expression of AR-target genes in enzalutamide-resistant cells*. Enzalutamide-resistant AR-expressing LNCaP cells (MR49F) were cultured and treated as indicated in panel **A**. RNA was isolated and the expression of AR-target gene FKBP5 was measured and normalized to GAPDH using real time PCR primers and probe. Growth assay in MR49F cells was performed using cell titer glo reagent. **C**. *UT-34 inhibits VCaP AR function and cell proliferation*. **Western blot**. Protein from LNCaP and VCaP cells was extracted and Western blot for AR and GAPDH was performed. **Bottom left**. VCaP cells were plated in growth medium. Medium was changed to 1% csFBS-containing medium and maintained in this medium for two days. Cells were treated for twenty-four hours, RNA was isolated, and expression of FKBP5 and TMPRSS2 was measured and normalized to GAPDH using real time PCR. **Bottom right**. VCaP cells were plated in growth medium. Medium was changed to

1%csFBS containing medium and treated. Cells were re-treated every third day and cell-titer glo assay was performed after nine days. **D**. *UT-34 inhibits PDX cell line PC346C AR function and cell proliferation*. **Western blot**. Protein from LNCaP and PC346C cells was extracted and Western blot for AR and GAPDH was performed. **Middle**. PC346C cells were plated in growth medium. Cells were treated for twenty-four hours in growth medium, RNA was isolated, and expression of FKBP5 was measured and normalized to GAPDH using real time PCR. **Bottom**. PC346C cells were plated in growth medium and treated. Cells were re-treated every third day and cell-titer glo assay was performed after six days. **E**. *Gene expression array in MR49F indicates UT-34 reverses the expression of genes regulated by R1881*. MR49F cells were maintained in charcoal-stripped serum-containing medium for 2 days and treated with vehicle, 0.1 nM R1881 alone or in combination with 10 μM of UT-34. RNA was isolated 24 hours after treatment and hybridized to Clariom D microarray. Genes that were differentially expressed by 1.5-fold and $q<0.05$ in R1881-treated samples compared to vehicle-treated samples are expressed in the heatmap to the left. The heatmap on the right shows the pattern of genes that were not regulated by R1881 (n=3-4/group). **F**. Ingenuity Pathway Analysis (IPA) demonstrating the top 5 canonical pathways and upstream regulators that were enriched in the UT-34 datasets. Enza-enzalutamide; Bical-bicalutamide; *=$p<0.05$; n=3-4/group.

**Figure 6**. **UT-34 inhibits the growth of androgen-dependent and enzalutamide-refractory castration-resistant prostate cancer xenografts**. **A**. *UT-34 inhibits growth of enzalutamide-resistant xenograft*. Enzalutamide-resistant LNCaP cells (MR49F) were implanted subcutaneously in NSG mice. Once the tumors reached 100-200 $mm^3$, the animals were castrated and the tumors were allowed to develop as castration-resistant tumors. Once the tumors reach

200-300 $mm^3$, the animals (n=8-10/group) were randomized and treated orally with vehicle (DMSO:PEG-300 (15:85)) or the indicated doses of UT-34. Tumor volume was measured twice weekly. Animals were sacrificed on day 30 and tumor weights were recorded. Values are represented as average ± S.E. * P<0.05; ** P<0.01. **B**. *UT-34 regresses tumors in immune-compromised rats*. VCaP prostate cancer cells (10 million) were mixed with 50% matrigel and implanted subcutaneously in SRG immune-compromised rats. Once the tumors reached 1000-3000 $mm^3$, the animals were castrated and the tumors were allowed to regrow as CRPC. Once the tumors grew after castration to 2000 $mm^3$, the animals were randomized (n=5-6/group) and treated orally with vehicle (DMSO+PEG-300 (15:85)), 30 mg/kg enzalutamide, or 60 mg/kg UT-34. Tumor volume was measured thrice weekly. Lines in the box indicate that the tumors in the treated groups are significantly different at p<0.01 to 0.001 from the vehicle group on the respective days. **C**. *UT-34 regresses the growth of enzalutamide-resistant VCaP tumors (MDVR)*. Tumor studies were conducted as indicated in panel B in SRG rats (n=5-6/group) with MDVR enzalutamide-resistant VCaP cells. **Western blot**. Protein extracts from the tumors were fractionated on a SDS-PAGE and were Western blotted with AR and GAPDH antibodies. **D**. *UT-34 regresses tumors in intact SRG rats*. MDVR cells (10 million) were implanted subcutaneously. Once the tumors reach above 2000 $mm^3$, the animals were randomized and treated orally with vehicle, 30 mg/kg enzalutamide, or 60 mg/kg UT-34. Individual animal data are presented. Serum PSA was measured using ELISA in three rats (one from each group) and represented in the bottom right panel. Western blots for AR and GAPDH are shown in the lower panel. **E**. *UT-34 dose-dependently inhibits MDVR tumor growth in intact SRG rats*. Xenograft studies were conducted in intact rats (n=5/group) as indicated above with a dose response of UT-34. Tumor volume was measured thrice weekly. Lines in the box indicate that the tumors in the

treated groups are significantly different at $p<0.01$ to 0.001 from the vehicle group on the respective days. Tumor weights and serum PSA were recorded at the end of the treatment period. Western blot is shown as a panel. Mpk-mg/kg body weight; Enza-enzalutamide; SRG rats: Sprague Dawley-Rag2:IL2rg KO rats.

## Supplementary Figure Legends

**Figure S1: UT-155 has poor metabolism and oral pharmacodynamic properties**. **A**. *UT-155 has no effect on seminal vesicles when administered orally*. C57BL6 mice weighing 20-25 grams (n=5/group) were treated orally with vehicle (15% DMSO+85% PEG-300) or the indicated doses of UT-155 or enzalutamide. Animals were sacrificed after 14 days of treatment and weights of seminal vesicles were recorded and normalized to body weight. The values are represented as percent change from vehicle-treated animals. *** $p<0.001$. **B**. *UT-155 has no effect on the growth of enzalutamide-resistant xenograft when administered orally*. Enzalutamide-resistant LNCaP cells (MR49F) were implanted subcutaneously in nude mice. Once the tumors reached 100-200 $mm^3$, the animals were castrated and the tumors were allowed to develop as castration-resistant tumors. Once the tumors reach 200-300 $mm^3$, the animals (n=8-10/group) were randomized and treated orally with vehicle (15% DMSO + 85% PEG-300) or 100 mg/kg UT-155. Tumor volume was measured twice weekly. **C**. *UT-155 has poor metabolism properties*. Liver microsomes from mouse (MLM) and human (HLM) were incubated with UT-155 as indicated in the methods and the amount of compound present at different points was identified using LC-MS/MS method. Data from both phase I and II metabolism are presented here. The data are represented as half-life ($T_{1/2}$) and intrinsic clearance ($Cl_{int}$).

**Figure S2. A. UT-34 does not down-regulate GR in MDA-MB-453 cells**. MDA-MB-453 cells that express AR and GR were treated as indicated in the figure. Cells were harvested 24 hours after treatment and Western blot for AR, GR, and GAPDH was performed. **B. UT-34-dependent AR-down-regulation is PAK and PKC independent**. LNCaP cells were plated in 60 mm dishes in growth medium. Medium was changed to RPMI+1%csFBS and maintained in this medium for two days. Cells were treated with 10 μM UT-34 alone or in combination with 1 μM PF3758309 (p21-activated kinase (PAK) inhibitor), or 10 μM chelerythrine chloride (protein kinase C (PKC) inhibitor) in the presence of 0.1 nM R1881. Twenty four hours after treatment, the cells were harvested, protein extracted, and Western blot for AR and GAPDH was performed. **C**. **UT-34-dependent AR degradation is independent of MDM2**. LNCaP cells were transfected with 100 nM non-specific or MDM2 siRNA. Twenty four hours after transfection, the cells were fed with growth medium and allowed to recover. Twenty-four hours later, the cells were treated with vehicle, 0.1 nM R1881, or a combination of 10 μM UT-34 and 0.1 nM R1881. Cells were harvested 24 hours after treatment, protein extracted, and Western blot for AR and GAPDH was performed. **Bottom**. RNA was extracted from cells transfected with non-specific or MDM2 siRNA and expression of MDM2 was measured and normalized to GAPDH by real time PCR. **D. UT-34 interacts with AR-NTD**. Steady state fluorescence emission spectra for purified AR-NTD (1 μM) in buffer or the presence of the osmolyte TMAO or the denaturant urea. Emission maxima for tryptophan (W) and tyrosine (Y) are indicated. Right Chart, AR-NTD purified protein (1 μM) and increasing concentrations of UT-34 were pre-incubated for at least 30 minutes and steady state fluorescence was measured. The emission spectra were all corrected for buffer and presence of UT-34 and plotted relative to tryptophan emission maximum set to 100.

**Figure S3. UT-34 does not inhibit proliferation of AR-negative cells**. **A**. PC-3, COS-7, and HEK-293 cells were plated in 1% charcoal-stripped serum-containing medium. Cells were treated with 1 or 10 μM of UT-34 in the presence of 0.1 nM R1881. Cells were re-treated three days later and the number of viable cells was measured by cell titer glo assay. **B**. UT-34 inhibits PSA expression and cell proliferation in enzalutamide-resistant VCaP (MDVR) cells. MDVR cells were plated in 1% charcoal stripped serum-containing medium. Cells were treated for 24 hours (left panel) or for 6 days (right panel). Expression of PSA was measured and normalized to GAPDH (left panel). Number of viable cells was measured by cell titer glo assay (right panel). * $p<0.05$. 34-UT-34; Enza-enzalutamide.

**Figure S4. A. UT-34 has appropriate pharmacokinetic and pharmacodynamics properties**. **A-B**. *UT-34 is stable up to 24 hours in rats*. Sprague Dawley rats (n=3-6/group) were dosed with the indicated doses of UT-34 once (A) or for 7 days (B). Blood was collected at the indicated time points on day 1 (A) or day 7 (B) and the amount of UT-34 remaining in the plasma was measured using LC-MS/MS method. **C**. *UT-34 inhibits seminal vesicles weight in mice and prostate and seminal vesicles weight in rats*. C57BL6 mice (left panel) weighing 20-25 grams (n=5/group) or Sprague Dawley rats (middle and right) weighing 200-250 grams (n=5/group) were treated orally with vehicle (15% DMSO+85% PEG-300) or the indicated doses of UT-34 or enzalutamide. Animals were sacrificed after 14 days (left and middle) or after 4 days (right) of treatment and weights of prostate and seminal vesicles were recorded and normalized to body weight. The values are represented as percent change from vehicle-treated animals. **D**. *UT-34 penetrates and gets accumulated in the tumors*. Drug was extracted from serum and tumors

shown in **Figure 6E** (30 mg/kg group) and UT-34 was measured using LC-MS/MS (n=4/group). **E**. *UT-34 inhibits proliferation and increases apoptosis*. Formalin-fixed tumor samples from **Figure 6E** were stained for Ki67 and TUNEL. Percent stained cells were quantified using an automated software. **F**. *UT-34 does not have agonistic activity in vivo at high doses*. C57BL/6 mice were castrated and treated orally for 30 days. After 30 days of treatment, animals were sacrificed and seminal vesicles weights were recorded and normalized to body weight. **Right panel**. UT-34 concentration in serum was measured by LC-MS/MS method. * $p<0.05$; ** $p<0.01$. mpk=mg/kg body weight. PK-pharmacokinetic; PD-pharmacodynamics.

**Figure S5. H&E staining of MDVR tumors from animals shown in figure 6E that were treated with vehicle or 30 mg/kg UT-34.**

**Table ST1**. **Binding and antagonistic properties of UT-34**. Binding of UT-34 to purified AR-LBD was determined by competitive radiolabeled binding assay. Transactivation assays were performed using wild-type or mutant ARs, and PR, GR, or MR. Cells were transfected with the indicated receptors, GRE-LUC, and CMV-renilla LUC. Cells were treated with a dose response between 1 pM and 10 μM and luciferase assay was performed 24 hours after treatment. N.B. No binding. AR-androgen receptor; PR-progesterone receptor; GR-glucocorticoid receptor; MR-mineralocorticoid receptor; T877A-Threonine 877 of AR mutated to alanine; W741L-tryptophan 741 of AR mutated to leucine.

**Table ST2**. **Metabolism properties of SARDs**. Liver microsomes from mouse (MLM), rat (RLM), and human (HLM) were incubated with UT-34 as indicated in the methods and the

amount of compound present at different points was identified using LC-MS/MS method. Data from both phase I and II metabolism are presented here. The data are represented as half-life ($T_{1/2}$) and intrinsic clearance ($Cl_{int}$).

**Table ST3**. **Pharmacokinetic properties of UT-34**. **A**. UT-34 is stable in rats, but not in mice. UT-34 (60 mg/kg) dissolved in 15% DMSO + 85% PEG-300 was administered orally to the indicated strains and species (n=3/group). Blood was collected 6 and 24 hours after dosing and the amount of UT-34 remaining in the serum was estimated using LC-MS/MS method.

**References**:


1. Miller KD, Siegel RL, Lin CC, Mariotto AB, Kramer JL, Rowland JH, *et al.* Cancer treatment and survivorship statistics, 2016. CA Cancer J Clin **2016**;66:271-89
2. de Bono JS, Logothetis CJ, Molina A, Fizazi K, North S, Chu L, *et al.* Abiraterone and increased survival in metastatic prostate cancer. N Engl J Med **2011**;364:1995-2005
3. Scher HI, Fizazi K, Saad F, Taplin ME, Sternberg CN, Miller K, *et al.* Increased survival with enzalutamide in prostate cancer after chemotherapy. N Engl J Med **2012**;367:1187-97
4. Smith MR, Kabbinavar F, Saad F, Hussain A, Gittelman MC, Bilhartz DL, *et al.* Natural history of rising serum prostate-specific antigen in men with castrate nonmetastatic prostate cancer. J Clin Oncol **2005**;23:2918-25
5. Chi KN, Hotte SJ, Yu EY, Tu D, Eigl BJ, Tannock I, *et al.* Randomized phase II study of docetaxel and prednisone with or without OGX-011 in patients with metastatic castration-resistant prostate cancer. J Clin Oncol **2010**;28:4247-54
6. Scher HI, Beer TM, Higano CS, Anand A, Taplin ME, Efstathiou E, *et al.* Antitumour activity of MDV3100 in castration-resistant prostate cancer: a phase 1-2 study. Lancet **2010**;375:1437-46
7. Ryan CJ, Smith MR, de Bono JS, Molina A, Logothetis CJ, de Souza P, *et al.* Abiraterone in metastatic prostate cancer without previous chemotherapy. N Engl J Med **2013**;368:138-48
8. Nadiminty N, Tummala R, Liu C, Yang J, Lou W, Evans CP, *et al.* NF-kappaB2/p52 induces resistance to enzalutamide in prostate cancer: role of androgen receptor and its variants. Mol Cancer Ther **2013**;12:1629-37
9. Korpal M, Korn JM, Gao X, Rakiec DP, Ruddy DA, Doshi S, *et al.* An F876L mutation in androgen receptor confers genetic and phenotypic resistance to MDV3100 (enzalutamide). Cancer Discov **2013**;3:1030-43
10. Antonarakis ES, Lu C, Wang H, Luber B, Nakazawa M, Roeser JC, *et al.* AR-V7 and resistance to enzalutamide and abiraterone in prostate cancer. N Engl J Med **2014**;371:1028-38

11. Lubahn DB, Joseph DR, Sullivan PM, Willard HF, French FS, Wilson EM. Cloning of human androgen receptor complementary DNA and localization to the X chromosome. Science **1988**;240:327-30
12. Yoshida T, Kinoshita H, Segawa T, Nakamura E, Inoue T, Shimizu Y, *et al.* Antiandrogen bicalutamide promotes tumor growth in a novel androgen-dependent prostate cancer xenograft model derived from a bicalutamide-treated patient. Cancer Res **2005**;65:9611-6
13. Clegg NJ, Wongvipat J, Joseph JD, Tran C, Ouk S, Dilhas A, *et al.* ARN-509: a novel antiandrogen for prostate cancer treatment. Cancer Res **2012**;72:1494-503
14. Balbas MD, Evans MJ, Hosfield DJ, Wongvipat J, Arora VK, Watson PA, *et al.* Overcoming mutation-based resistance to antiandrogens with rational drug design. Elife **2013**;2:e00499
15. Hornberg E, Ylitalo EB, Crnalic S, Antti H, Stattin P, Widmark A, *et al.* Expression of androgen receptor splice variants in prostate cancer bone metastases is associated with castration-resistance and short survival. PLoS One **2011**;6:e19059
16. Zhang G, Liu X, Li J, Ledet E, Alvarez X, Qi Y, *et al.* Androgen receptor splice variants circumvent AR blockade by microtubule-targeting agents. Oncotarget **2015**;6:23358-71
17. Cheng HH, Gulati R, Azad A, Nadal R, Twardowski P, Vaishampayan UN, *et al.* Activity of enzalutamide in men with metastatic castration-resistant prostate cancer is affected by prior treatment with abiraterone and/or docetaxel. Prostate Cancer Prostatic Dis **2015**;18:122-7
18. Mezynski J, Pezaro C, Bianchini D, Zivi A, Sandhu S, Thompson E, *et al.* Antitumour activity of docetaxel following treatment with the CYP17A1 inhibitor abiraterone: clinical evidence for cross-resistance? Ann Oncol **2012**;23:2943-7
19. Liu C, Zhu Y, Lou W, Cui Y, Evans CP, Gao AC. Inhibition of constitutively active Stat3 reverses enzalutamide resistance in LNCaP derivative prostate cancer cells. Prostate **2014**;74:201-9
20. Culig Z, Bartsch G, Hobisch A. Interleukin-6 regulates androgen receptor activity and prostate cancer cell growth. Mol Cell Endocrinol **2002**;197:231-8
21. McClelland RA, Manning DL, Gee JM, Anderson E, Clarke R, Howell A, *et al.* Effects of short-term antiestrogen treatment of primary breast cancer on estrogen receptor mRNA and protein expression and on estrogen-regulated genes. Breast Cancer Res Treat **1996**;41:31-41
22. Bihani T, Patel HK, Arlt H, Tao N, Jiang H, Brown JL, *et al.* Elacestrant (RAD1901), a Selective Estrogen Receptor Degrader (SERD), Has Antitumor Activity in Multiple ER+ Breast Cancer Patient-derived Xenograft Models. Clin Cancer Res **2017**;23:4793-804
23. Watson PA, Chen YF, Balbas MD, Wongvipat J, Socci ND, Viale A, *et al.* Constitutively active androgen receptor splice variants expressed in castration-resistant prostate cancer require full-length androgen receptor. Proc Natl Acad Sci U S A **2010**;107:16759-65
24. Xu D, Zhan Y, Qi Y, Cao B, Bai S, Xu W, *et al.* Androgen Receptor Splice Variants Dimerize to Transactivate Target Genes. Cancer Res **2015**;75:3663-71
25. Raina K, Lu J, Qian Y, Altieri M, Gordon D, Rossi AM, *et al.* PROTAC-induced BET protein degradation as a therapy for castration-resistant prostate cancer. Proc Natl Acad Sci U S A **2016**;113:7124-9

26. Tang YQ, Han BM, Yao XQ, Hong Y, Wang Y, Zhao FJ, *et al.* Chimeric molecules facilitate the degradation of androgen receptors and repress the growth of LNCaP cells. Asian J Androl **2009**;11:119-26
27. Ponnusamy S, Coss CC, Thiyagarajan T, Watts K, Hwang DJ, He Y, *et al.* Novel Selective Agents for the Degradation of Androgen Receptor Variants to Treat Castration-Resistant Prostate Cancer. Cancer Res **2017**;77:6282-98
28. Hwang DJ, He Y, Ponnusamy S, Mohler ML, Thiyagarajan T, McEwan IJ, *et al.* A New Generation of Selective Androgen Receptor Degraders: Our Initial Design, Synthesis, and Biological Evaluation of New Compounds with Enzalutamide-Resistant Prostate Cancer Activity. J Med Chem **2018**
29. Andersen RJ, Mawji NR, Wang J, Wang G, Haile S, Myung JK, *et al.* Regression of castrate-recurrent prostate cancer by a small-molecule inhibitor of the amino-terminus domain of the androgen receptor. Cancer Cell **2010**;17:535-46
30. Krause WC, Shafi AA, Nakka M, Weigel NL. Androgen receptor and its splice variant, AR-V7, differentially regulate FOXA1 sensitive genes in LNCaP prostate cancer cells. Int J Biochem Cell Biol **2014**;54:49-59
31. Shafi AA, Putluri V, Arnold JM, Tsouko E, Maity S, Roberts JM, *et al.* Differential regulation of metabolic pathways by androgen receptor (AR) and its constitutively active splice variant, AR-V7, in prostate cancer cells. Oncotarget **2015**;6:31997-2012
32. Hu R, Dunn TA, Wei S, Isharwal S, Veltri RW, Humphreys E, *et al.* Ligand-independent androgen receptor variants derived from splicing of cryptic exons signify hormone-refractory prostate cancer. Cancer Res **2009**;69:16-22
33. Toren PJ, Kim S, Pham S, Mangalji A, Adomat H, Guns ES, *et al.* Anticancer activity of a novel selective CYP17A1 inhibitor in preclinical models of castrate-resistant prostate cancer. Mol Cancer Ther **2015**;14:59-69
34. Marques RB, Aghai A, de Ridder CMA, Stuurman D, Hoeben S, Boer A, *et al.* High Efficacy of Combination Therapy Using PI3K/AKT Inhibitors with Androgen Deprivation in Prostate Cancer Preclinical Models. Eur Urol **2015**;67:1177-85
35. Marques RB, Erkens-Schulze S, de Ridder CM, Hermans KG, Waltering K, Visakorpi T, *et al.* Androgen receptor modifications in prostate cancer cells upon long-termandrogen ablation and antiandrogen treatment. Int J Cancer **2005**;117:221-9
36. Narayanan R, Coss CC, Yepuru M, Kearbey JD, Miller DD, Dalton JT. Steroidal androgens and nonsteroidal, tissue-selective androgen receptor modulator, S-22, regulate androgen receptor function through distinct genomic and nongenomic signaling pathways. Mol Endocrinol **2008**;22:2448-65
37. Yepuru M, Wu Z, Kulkarni A, Yin F, Barrett CM, Kim J, *et al.* Steroidogenic enzyme AKR1C3 is a novel androgen receptor-selective coactivator that promotes prostate cancer growth. Clin Cancer Res **2013**;19:5613-25
38. Scheller A, Hughes E, Golden KL, Robins DM. Multiple receptor domains interact to permit, or restrict, androgen-specific gene activation. J Biol Chem **1998**;273:24216-22
39. Callewaert L, Van Tilborgh N, Claessens F. Interplay between two hormone-independent activation domains in the androgen receptor. Cancer Res **2006**;66:543-53
40. Callewaert L, Verrijdt G, Haelens A, Claessens F. Differential effect of small ubiquitin-like modifier (SUMO)-ylation of the androgen receptor in the control of cooperativity on selective versus canonical response elements. Mol Endocrinol **2004**;18:1438-49

41. James AJ, Agoulnik IU, Harris JM, Buchanan G, Tilley WD, Marcelli M, *et al.* A novel androgen receptor mutant, A748T, exhibits hormone concentration-dependent defects in nuclear accumulation and activity despite normal hormone-binding affinity. Mol Endocrinol **2002**;16:2692-705
42. Reid J, Murray I, Watt K, Betney R, McEwan IJ. The androgen receptor interacts with multiple regions of the large subunit of general transcription factor TFIIF. J Biol Chem **2002**;277:41247-53
43. Houtman R, de Leeuw R, Rondaij M, Melchers D, Verwoerd D, Ruijtenbeek R, *et al.* Serine-305 phosphorylation modulates estrogen receptor alpha binding to a coregulator peptide array, with potential application in predicting responses to tamoxifen. Mol Cancer Ther **2012**;11:805-16
44. Cato L, de Tribolet-Hardy J, Lee I, Rottenberg JT, Coleman I, Melchers D, *et al.* ARv7 Represses Tumor-Suppressor Genes in Castration-Resistant Prostate Cancer. Cancer Cell **2019**;35:401-13 e6
45. Narayanan R, Yepuru M, Szafran AT, Szwarc M, Bohl CE, Young NL, *et al.* Discovery and mechanistic characterization of a novel selective nuclear androgen receptor exporter for the treatment of prostate cancer. Cancer Res **2010**;70:842-51
46. Buchanan G, Birrell SN, Peters AA, Bianco-Miotto T, Ramsay K, Cops EJ, *et al.* Decreased androgen receptor levels and receptor function in breast cancer contribute to the failure of response to medroxyprogesterone acetate. Cancer Res **2005**;65:8487-96
47. Tilley WD, Marcelli M, McPhaul MJ. Expression of the human androgen receptor gene utilizes a common promoter in diverse human tissues and cell lines. J Biol Chem **1990**;265:13776-81
48. Mitchell S, Abel P, Madaan S, Jeffs J, Chaudhary K, Stamp G, *et al.* Androgen-dependent regulation of human MUC1 mucin expression. Neoplasia **2002**;4:9-18
49. Robinson JL, Macarthur S, Ross-Innes CS, Tilley WD, Neal DE, Mills IG, *et al.* Androgen receptor driven transcription in molecular apocrine breast cancer is mediated by FoxA1. EMBO J **2011**;30:3019-27
50. Hartig PC, Bobseine KL, Britt BH, Cardon MC, Lambright CR, Wilson VS, *et al.* Development of two androgen receptor assays using adenoviral transduction of MMTV-luc reporter and/or hAR for endocrine screening. Toxicol Sci **2002**;66:82-90
51. Patek S, Willder J, Heng J, Taylor B, Horgan P, Leung H, *et al.* Androgen receptor phosphorylation status at serine 578 predicts poor outcome in prostate cancer patients. Oncotarget **2017**;8:4875-87
52. Liu T, Li Y, Gu H, Zhu G, Li J, Cao L, *et al.* p21-Activated kinase 6 (PAK6) inhibits prostate cancer growth via phosphorylation of androgen receptor and tumorigenic E3 ligase murine double minute-2 (Mdm2). J Biol Chem **2013**;288:3359-69
53. Civiero L, Cogo S, Kiekens A, Morganti C, Tessari I, Lobbestael E, *et al.* PAK6 Phosphorylates 14-3-3gamma to Regulate Steady State Phosphorylation of LRRK2. Front Mol Neurosci **2017**;10:417
54. Eckly-Michel AE, Le Bec A, Lugnier C. Chelerythrine, a protein kinase C inhibitor, interacts with cyclic nucleotide phosphodiesterases. Eur J Pharmacol **1997**;324:85-8
55. Vummidi Giridhar P, Williams K, VonHandorf AP, Deford PL, Kasper S. Constant Degradation of the Androgen Receptor by MDM2 Conserves Prostate Cancer Stem Cell Integrity. Cancer Res **2019**;79:1124-37

56. Reid J, Kelly SM, Watt K, Price NC, McEwan IJ. Conformational analysis of the androgen receptor amino-terminal domain involved in transactivation. Influence of structure-stabilizing solutes and protein-protein interactions. J Biol Chem **2002**;277:20079-86
57. Trevino LS, Bolt MJ, Grimm SL, Edwards DP, Mancini MA, Weigel NL. Differential Regulation of Progesterone Receptor-Mediated Transcription by CDK2 and DNA-PK. Mol Endocrinol **2016**;30:158-72
58. Linja MJ, Savinainen KJ, Saramaki OR, Tammela TL, Vessella RL, Visakorpi T. Amplification and overexpression of androgen receptor gene in hormone-refractory prostate cancer. Cancer Res **2001**;61:3550-5
59. Visakorpi T, Hyytinen E, Koivisto P, Tanner M, Keinanen R, Palmberg C, *et al.* In vivo amplification of the androgen receptor gene and progression of human prostate cancer. Nat Genet **1995**;9:401-6
60. Waltering KK, Helenius MA, Sahu B, Manni V, Linja MJ, Janne OA, *et al.* Increased expression of androgen receptor sensitizes prostate cancer cells to low levels of androgens. Cancer Res **2009**;69:8141-9
61. Tran C, Ouk S, Clegg NJ, Chen Y, Watson PA, Arora V, *et al.* Development of a second-generation antiandrogen for treatment of advanced prostate cancer. Science **2009**;324:787-90
62. Kawata H, Arai S, Nakagawa T, Ishikura N, Nishimoto A, Yoshino H, *et al.* Biological properties of androgen receptor pure antagonist for treatment of castration-resistant prostate cancer: optimization from lead compound to CH5137291. Prostate **2011**;71:1344-56
63. Makkonen H, Kauhanen M, Jaaskelainen T, Palvimo JJ. Androgen receptor amplification is reflected in the transcriptional responses of Vertebral-Cancer of the Prostate cells. Mol Cell Endocrinol **2011**;331:57-65
64. Shibata N, Nagai K, Morita Y, Ujikawa O, Ohoka N, Hattori T, *et al.* Development of Protein Degradation Inducers of Androgen Receptor by Conjugation of Androgen Receptor Ligands and Inhibitor of Apoptosis Protein Ligands. J Med Chem **2018**;61:543-75
65. Pollock JA, Wardell SE, Parent AA, Stagg DB, Ellison SJ, Alley HM, *et al.* Inhibiting androgen receptor nuclear entry in castration-resistant prostate cancer. Nat Chem Biol **2016**;12:795-801
66. Czerniak R. Gender-based differences in pharmacokinetics in laboratory animal models. Int J Toxicol **2001**;20:161-3
67. Chang SC, Das K, Ehresman DJ, Ellefson ME, Gorman GS, Hart JA, *et al.* Comparative pharmacokinetics of perfluorobutyrate in rats, mice, monkeys, and humans and relevance to human exposure via drinking water. Toxicol Sci **2008**;104:40-53

# Figure 1

**A**

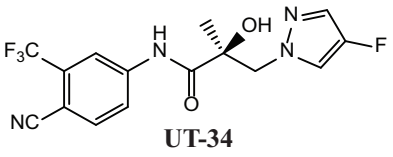


**UT-34**

**B**

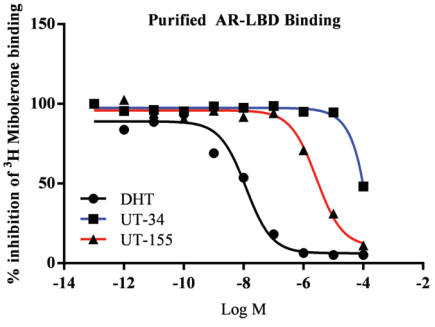


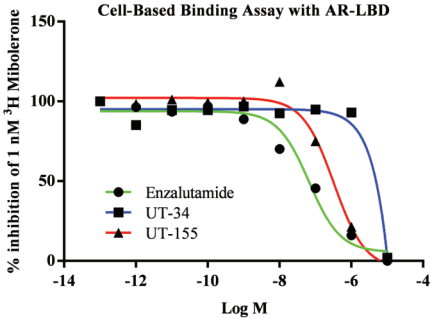


**C**

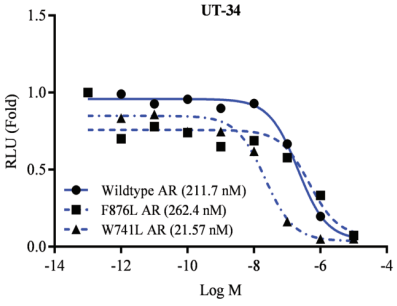


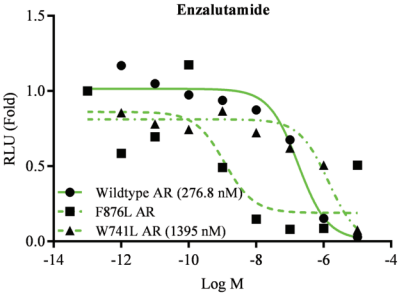


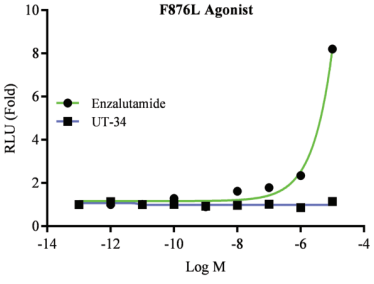

# Figure 2

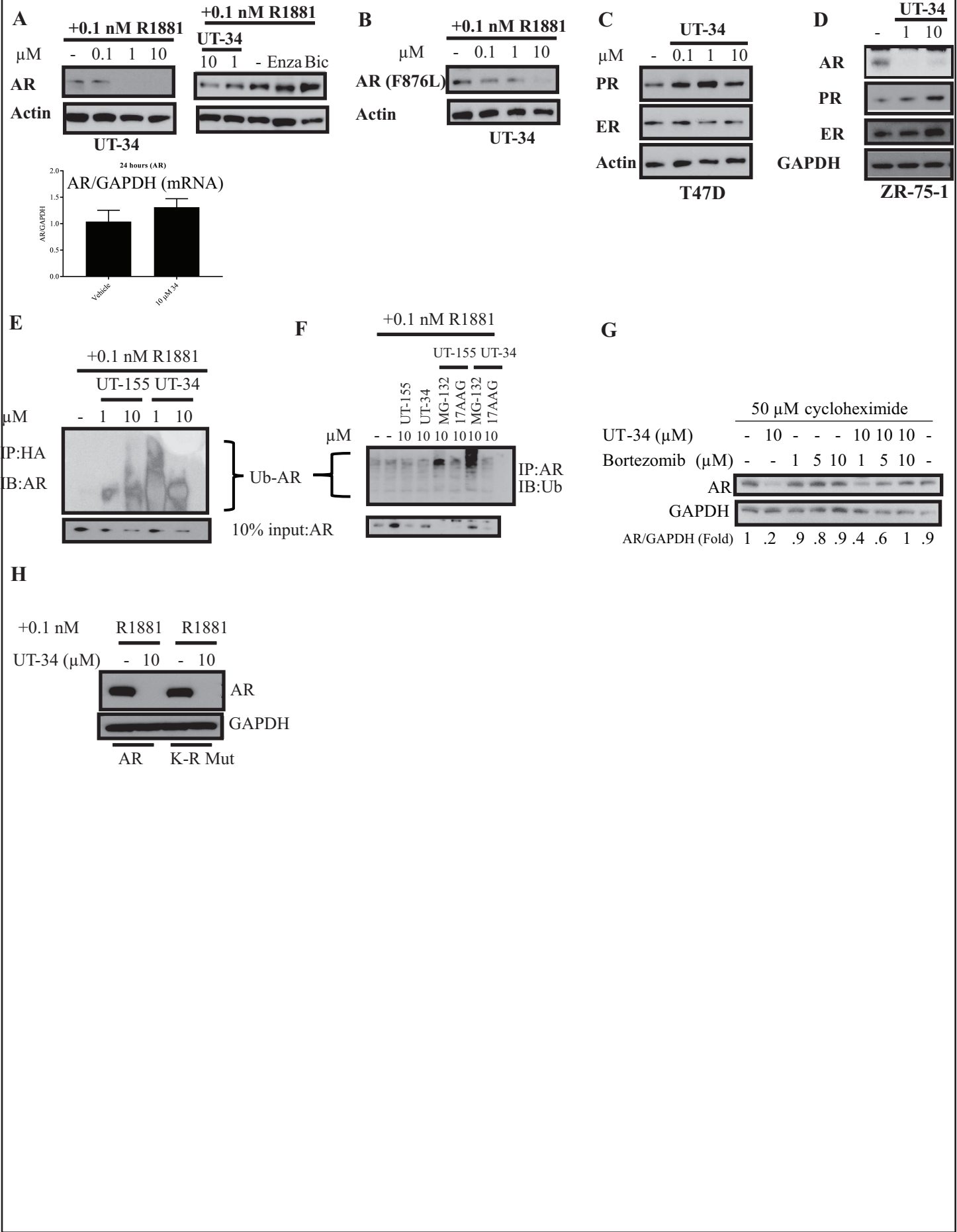
A
+0.1 nM R1881
μM - 0.1 1 10
AR
Actin
UT-34
+0.1 nM R1881
UT-34
10 1 - Enza Bic
24 hours (AR)
AR/GAPDH (mRNA)
AR/GAPDH
Vehicle
10 μM 34
B
+0.1 nM R1881
μM - 0.1 1 10
AR (F876L)
Actin
UT-34
C
UT-34
μM - 0.1 1 10
PR
ER
Actin
T47D
D
UT-34
- 1 10
AR
PR
ER
GAPDH
ZR-75-1
E
+0.1 nM R1881
UT-155 UT-34
μM - 1 10 1 10
IP:HA
IB:AR
Ub-AR
10% input:AR
F
+0.1 nM R1881
UT-155 UT-34
UT-155
UT-34
MG-132
17AAG
MG-132
17AAG
μM - - 10 10 10 10 10 10
IP:AR
IB:Ub
G
50 μM cycloheximide
UT-34 (μM) - 10 - - - 10 10 10 -
Bortezomib (μM) - - 1 5 10 1 5 10 -
AR
GAPDH
AR/GAPDH (Fold) 1 .2 .9 .8 .9 .4 .6 1 .9
H
+0.1 nM R1881 R1881 R1881
UT-34 (μM) - 10 - 10
AR
GAPDH
AR K-R Mut

# Figure 3

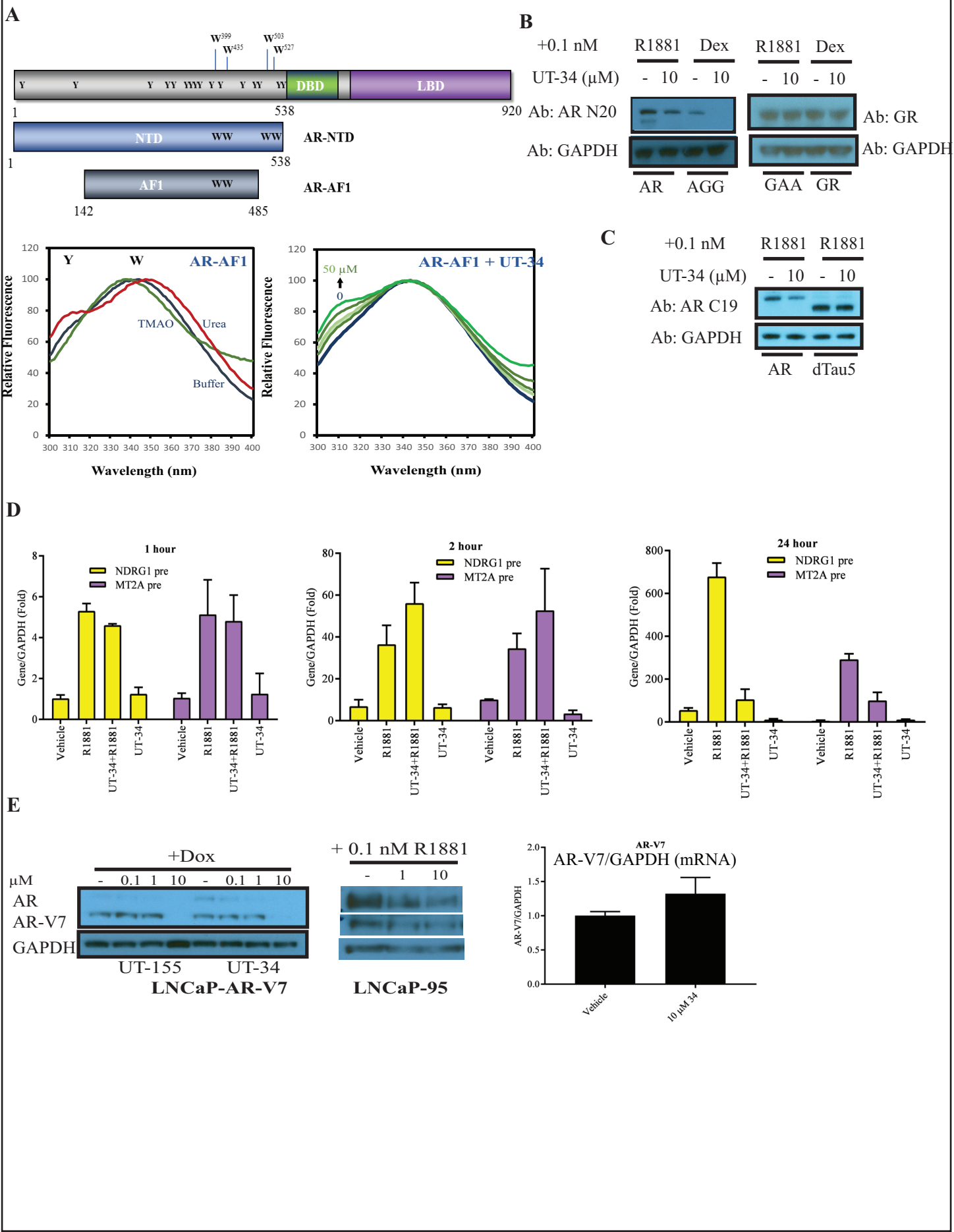
A
W399
W435
W503
W527
DBD
LBD
1
538
920
NTD
AR-NTD
AF1
AR-AF1
142
485
B
+0.1 nM
R1881
Dex
UT-34 (μM)
Ab: AR N20
Ab: GAPDH
Ab: GR
AR
AGG
GAA
GR
C
Ab: AR C19
dTau5
AR-AF1
TMAO
Urea
Buffer
AR-AF1 + UT-34
50 μM
0
Relative Fluorescence
Wavelength (nm)
D
1 hour
2 hour
24 hour
NDRG1 pre
MT2A pre
Gene/GAPDH (Fold)
Vehicle
R1881
UT-34+R1881
UT-34
E
+Dox
μM
AR
AR-V7
GAPDH
UT-155
UT-34
LNCaP-AR-V7
+ 0.1 nM R1881
LNCaP-95
AR-V7
AR-V7/GAPDH (mRNA)
AR-V7/GAPDH
Vehicle
10 μM 34

# Figure 4

**A**

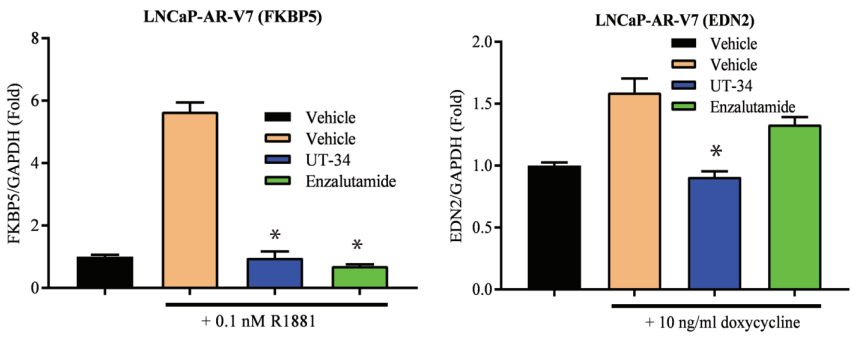


**B**

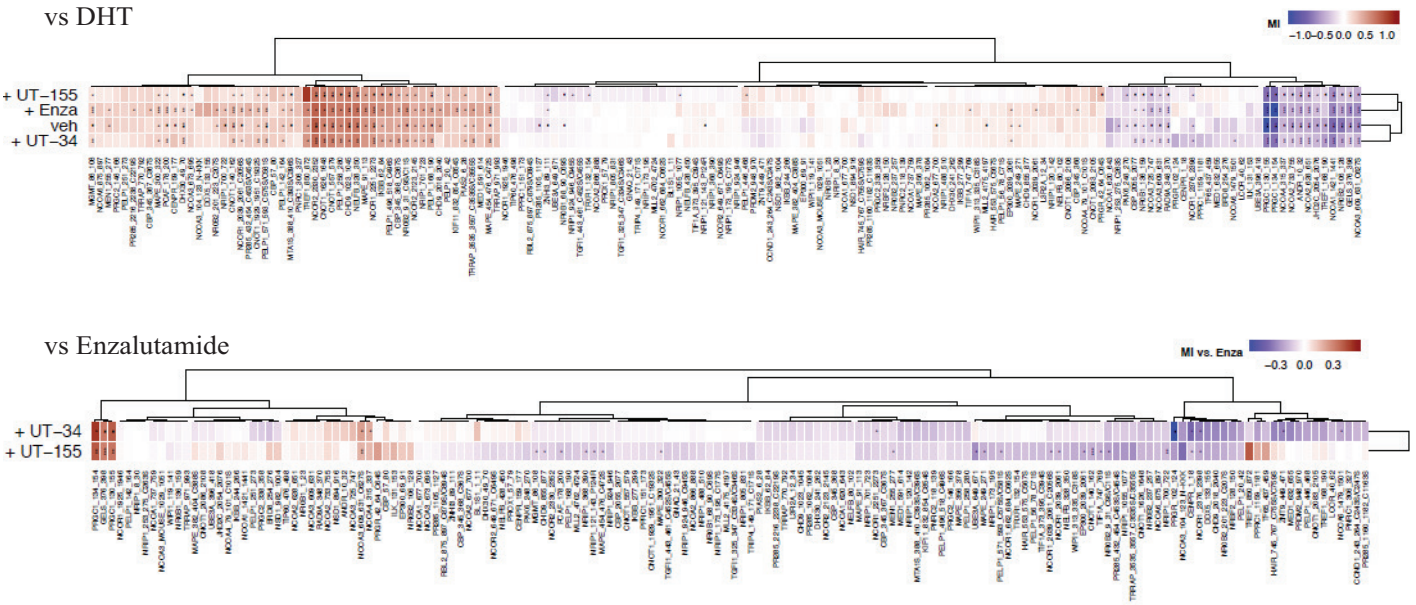


| | | |
|---|---|---|
| NCoA3 | NRIP | PRGR |
| NCoA4 | MEN1 | CENPR |
| MGMT | UBE3A | ZNT9 |
| CHD9 | NCoR1 | NCoA6 |
| PCAF | EP300 | |
| NRIP1 | cNOT1 | |
| MAPE | TIF1A | |
| NRIP | NROB2 | |

**List of proteins statistically different in SARDs compared to Enzalutamide**

# Figure 5

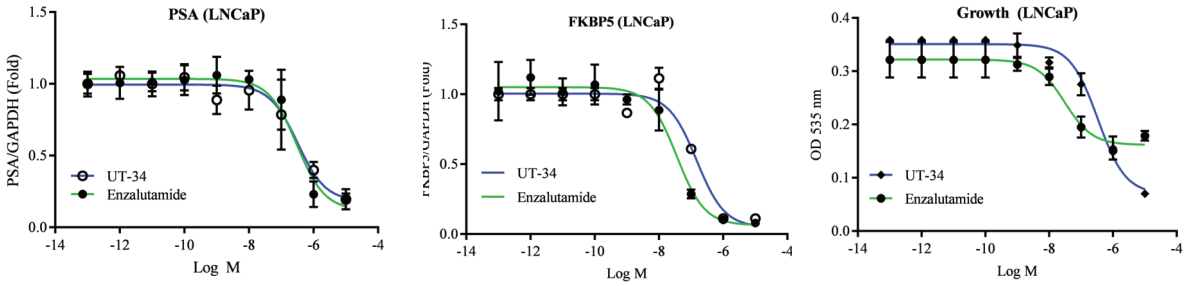


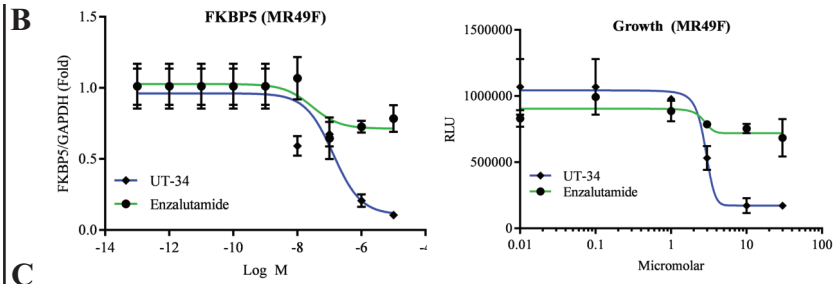


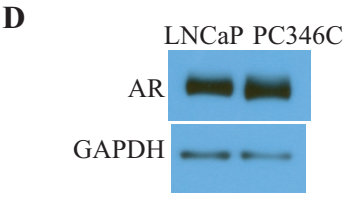


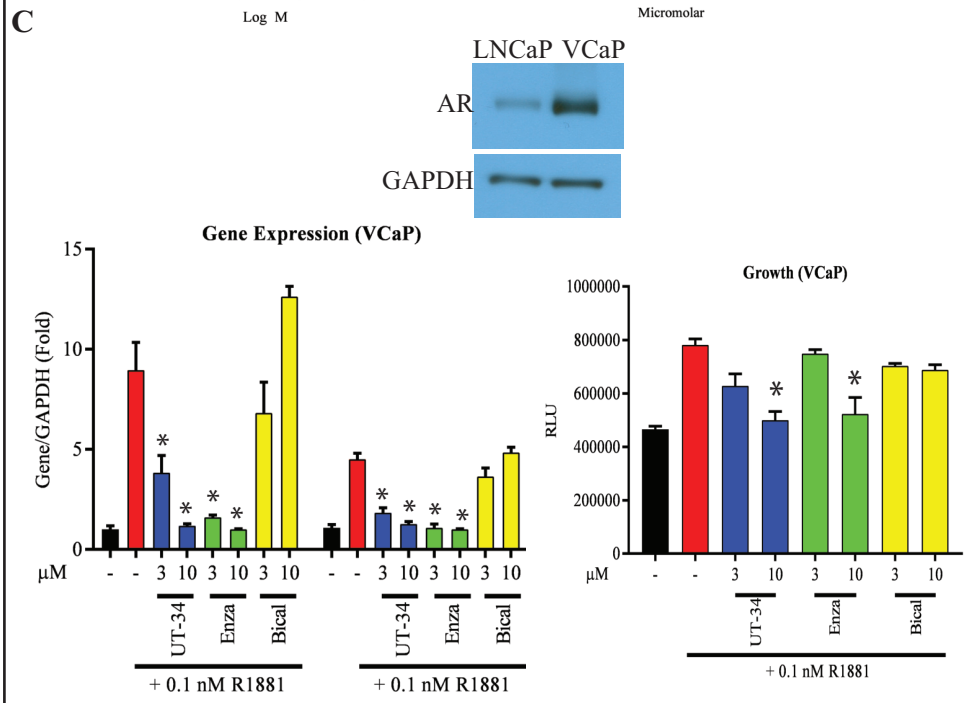


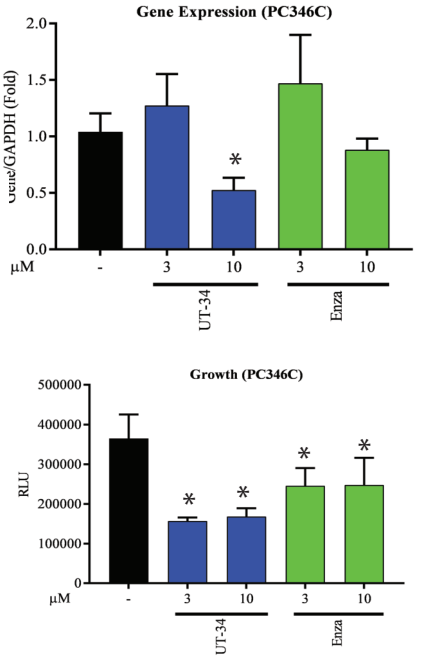


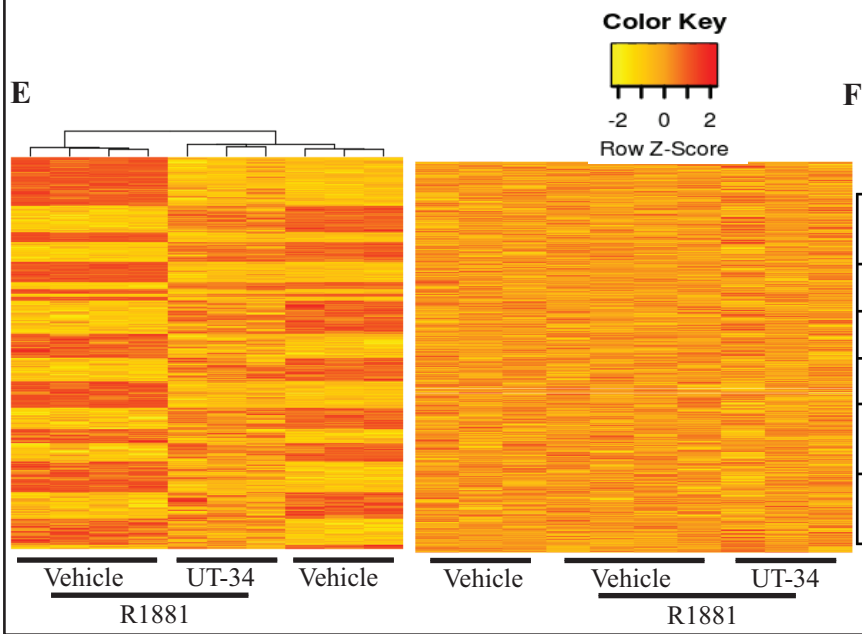


F

| Top 5 canonical pathways | Top 5 upstream regulators |
|---|---|
| Cholesterol biosynthesis I | Metribolone |
| Cholesterol biosynthesis II | Dihydrotestosterone |
| Cholesterol biosynthesis III | B-estradiol |
| Super pathway of cholesterol biosynthesis | Androgen receptor |
| UDP-N-acetyl-D-galactosamine II | Sterol |

# Figure 6

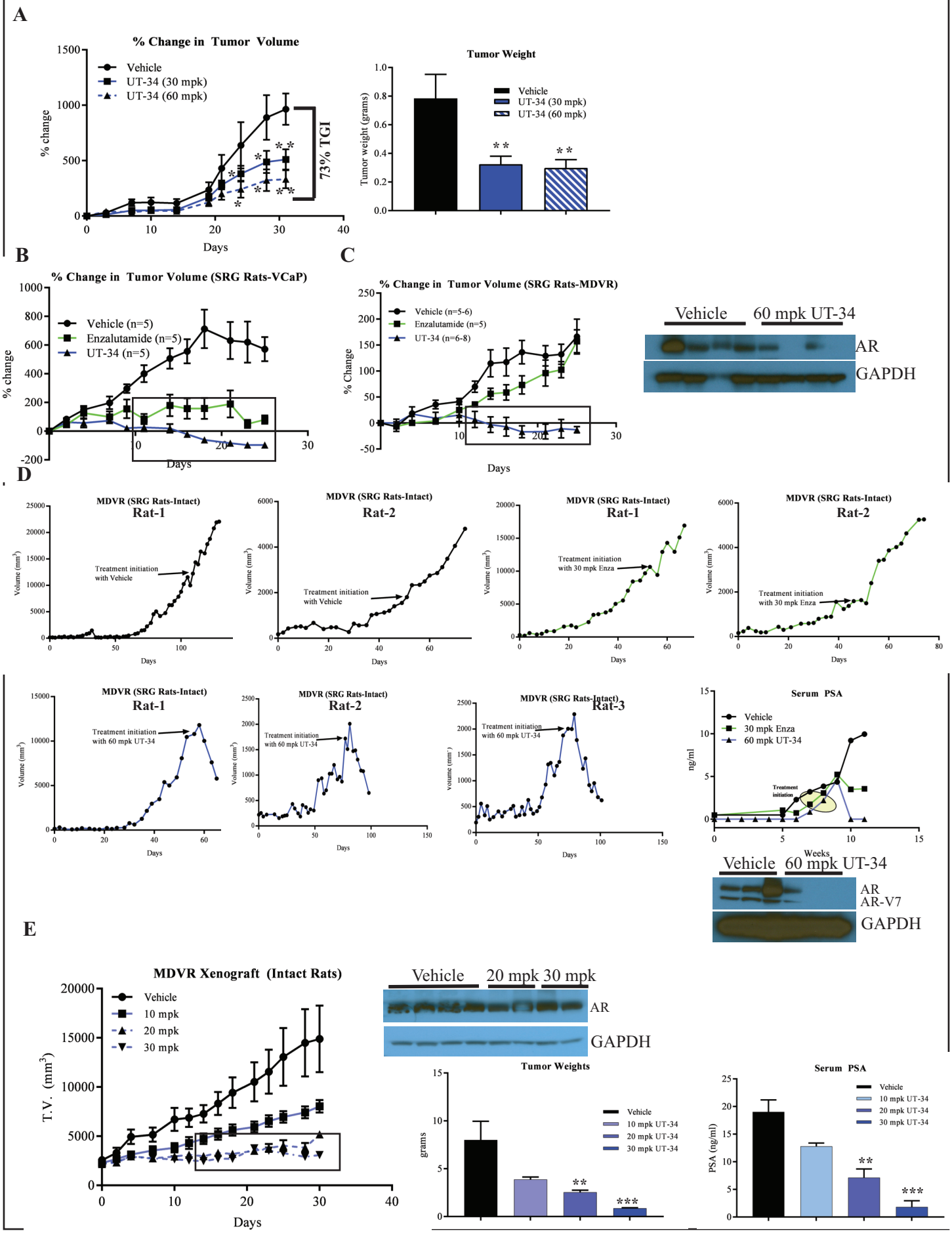
A
% Change in Tumor Volume
Vehicle
UT-34 (30 mpk)
UT-34 (60 mpk)
% change
Days
73% TGI
Tumor Weight
Tumor weight (grams)
B
% Change in Tumor Volume (SRG Rats-VCaP)
Vehicle (n=5)
Enzalutamide (n=5)
UT-34 (n=5)
C
% Change in Tumor Volume (SRG Rats-MDVR)
Vehicle (n=5-6)
Enzalutamide (n=5)
UT-34 (n=6-8)
Vehicle
60 mpk UT-34
AR
GAPDH
D
MDVR (SRG Rats-Intact)
Rat-1
Rat-2
Rat-3
Volume (mm3)
Treatment initiation with Vehicle
Treatment initiation with 30 mpk Enza
Treatment initiation with 60 mpk UT-34
Serum PSA
Vehicle
30 mpk Enza
60 mpk UT-34
ng/ml
Weeks
Vehicle
60 mpk UT-34
AR
AR-V7
GAPDH
E
MDVR Xenograft (Intact Rats)
Vehicle
10 mpk
20 mpk
30 mpk
T.V. (mm3)
Vehicle
20 mpk
30 mpk
AR
GAPDH
Tumor Weights
grams
Vehicle
10 mpk UT-34
20 mpk UT-34
30 mpk UT-34
Serum PSA
PSA (ng/ml)